DEVELOPMENT OF SLIDING VANE EXPANDERS FOR A MICRO–SCALE ORC SYSTEM

BY

WORAKIT SUANKRAMDEE

A THESIS SUBMITTED IN PARTIAL FULFILLMENT OF THE REQUIREMENTS FOR THE DEGREE OF MASTER OF SCIENCE (ENGINEERING AND TECHNOLOGY)

SIRINDHORN INTERNATIONAL INSTITUTE OF TECHNOLOGY

THAMMASAT UNIVERSITY

ACADEMIC YEAR 2016

DEVELOPMENT OF SLIDING VANE EXPANDERS FOR A MICRO–SCALE ORC SYSTEM

BY

WORAKIT SUANKRAMDEE

A THESIS SUBMITTED IN PARTIAL FULFILLMENT OF THE REQUIREMENTS FOR THE DEGREE OF MASTER OF SCIENCE (ENGINEERING AND TECHNOLOGY)

SIRINDHORN INTERNATIONAL INSTITUTE OF TECHNOLOGY

THAMMASAT UNIVERSITY

ACADEMIC YEAR 2016

DEVELOPMENT OF SLIDING VANE EXPANDERS FOR
A MICRO–SCALE ORC SYSTEM

A Thesis Presented

By

WORAKIT SUANKRAMDEE

Submitted to
Sirindhorn International Institute of Technology
Thammasat University
In partial fulfillment of the requirements for the degree of
MASTER OF SCIENCE (ENGINEERING AND TECHNOLOGY)

Approved as to style and content by

Advisor and Chairperson of Thesis Committee _____
(Prof. Dr. Satha Aphornratana)

Committee Member and
Chairperson of Examination Committee _____
(Col. Asst. Prof. Dr. Anotai Suksangpanomrung)

Committee Member _____
(Assoc. Prof. Dr. Bundit Limmeechokchai)

Committee Member _____
(Dr. Thunyaseth Sethaput)

JULY 2017

Abstract

DEVELOPMENT OF SLIDING VANE EXPANDERS FOR
A MICRO–SCALE ORC SYSTEM

by

WORAKIT SUANKRAMDEE

Bachelor of Engineering, (Mechanical Engineering), Sirindhorn International Institute of Technology, Thammasat University, 2014

The Organic Rankine Cycle (ORC) is one of the heat engines which can utilize low−grade heat to produce useful mechanical shaft power. Furthermore, it can be used for producing electricity, or other useful works. The working principle of the ORC is similar to the traditional steam Rankine cycle but there is a difference in the working fluid used. The organic substance is used as the working fluid. Most of the organic substances have a lower boiling point at atmospheric pressure compared to water. Hence, at identical temperature, a higher saturation pressure for the organic substance is made possible. This has high potential to drive the turbine.

In the ORC system, the expander is a key role component on the system. Each type of expander has its own characteristic which is suitable for each ORC system capacity. The expanders used for ORC system can be categorized into two types: velocity–type; and volume–type. The volume–type expander are more practical for the micro–scale ORC system because they are characterized by lower flow rates, higher pressure ratio, and much lower rotational speeds compared with the velocity–type expander. The volume–type expanders can tolerate two–phase flow conditions, which may appear at the end of expansion in some operating condition.

The sliding vane expander, which is one of the volume–type expanders, is selected to apply with a micro–scale ORC system. This expander is very attractive in applications where low initial cost and high power density are much more important than efficiency. Even though its efficiency is relatively low compared to the other types,

it has relatively simple structure and consists of a comparatively small number of low cost parts.

This study focused on the development of sliding vane expanders (2AM and 1AM expanders). They were modified from two commercially available air motor (GAST 2AM and GAST 1AM air motor). The 2AM and 1AM expanders were totally manufactured in–house at the SIIT mechanical engineering laboratory. They were redesigned while keeping the original essential dimensions and operating principles of the original GAST air motors. They were modified so that the units were leak proof and suitable to use as expenders for a micro scale ORC.

The sliding vane expander was successfully developed and tested with a micro–scale ORC system. The expander was workable with the system at the various operating conditions. The experimental results show that the expander provided an acceptable performance.

Keywords: Sliding vane expander, Organic Rankine Cycle, Waste heat recovery

Acknowledgements

The author would like to express his deep sense of gratitude and appreciation to his advisor, Prof. Dr. Satha Aphornratana for his invaluable of time, advice, patience, motivation and helpful guidance throughout this thesis study. Without his guidance and persistent help, this thesis would not have been possible.

He also wishes to faithfully acknowledge Assoc. Prof. Dr. Bundit Limmeechokchai, Dr. Thunyaseth Sethaput, and Col. Asst. Prof. Dr. Anotai Suksangpanomrung for kindly consenting to be members of the thesis examination committee, as well as for sharing their valuable time and providing very useful advice.

Thanks to the Sirindhorn International Institute of Technology (SIIT) for giving an opportunity to undertake the M.Sc. course.

He wishes to express his sincere appreciation to Mr. Tongchana Thongtip for his kind advice, research experiences, and contributions to this research. Special thanks to his colleagues, Mr. Kanchit Pawananont, and Mr. Borirak Kitrattana for their research comments, technical advice and mostly, grateful working environment. And also, Mr. Nikhom Meedet for his technical assistance.

Last but not least, he sincerely thanks his family, Pol.Maj.Gen. Woranit Suankramdee, Pol.Lt. Marisa Singkatera, and Mr. Worapot Suankramdee, for their endless support and encouragement throughout many difficult situations during the period of this study at Sirindhorn International Institute of Technology (SIIT), Thammasat University.

Table of Contents

List of Figures

Figures **Page**

Figures **Page**

List of Tables

Nomenclatures

ORC	Organic Rankine Cycle
F	Force (N)
h	Enthalpy of the working fluid (kJ/kg)
$\dot{m}$	Mass flow of the working fluid (kg/sec)
n	Rotational speed of the expander (rpm)
P	Pressure of the working fluid (kPa)
$\dot{Q}$	Heat (kW)
r	Radius of the pulley (m)
$\dot{W}$	Power (kW)

Greek Letters

η	Thermal efficiency of the ORC system (%)
τ	Torque (N·m)
υ	Specific volume of the working fluid (m^3/kg)

Subscripts

sys	ORC system
gen	Condition at vapour generator
con	Condition at condenser
ex	Condition at expander
f	Saturated liquid
g	Saturated vapour

Chapter 1
Introduction

In the power generation process, the traditional steam Rankine cycle has been used to produce electricity. In such a system, heat (available from various sources such as burning coal or natural gas, exhaust of the gas turbine generator, and etc.) is used to produce a high pressure steam to drive a turbine for producing mechanical work for the AC generator. The heat required for the steam boiler is at relatively high temperature, usually not below 300°C. Therefore, low−grade industrial waste heat is not efficient for operation.

The Organic Rankine Cycle (ORC) is one of the heat engines which can utilize low−grade heat to produce useful mechanical shaft power. It can convert low–grade heat (available from: renewable energy sources such as solar thermal, geothermal, or biomass firing; or waste heat from the process such as industrial process, or the exhaust gas from the engine) to mechanical work. Furthermore, it can be used for producing electricity, or other useful works. The working principle of the ORC is similar to the traditional steam Rankine cycle but there is a difference in the working fluid used. Organic substance such as HCs (Hydrocarbons, butane, and propane), HFCs (Hydrofluorocarbons, HFC134a, and HFC245fa), and HCFCs (Hydrochlorofluorocarbons, HCFC123 and HCFC141b) are used as the working fluid [Bao and Zhao, 2013]. The organic substance is also used in the refrigeration cycle as a refrigerant (R134a). Most of the organic substances have a lower boiling point at atmospheric pressure compared to water. Hence, at identical temperature, a higher saturation pressure for the organic substance is made possible. This has high potential to drive the turbine.

The ORC system was first developed more than a century ago. The first ORC engine was invented by Frank Ofeldt in the 1880s. The working fluid used was naphtha and the engine was used to power a small boat. At that time, the government required a license to run steam engines but did not require one when boiled naphtha. Therefore, with the use of this naphtha engine, the boat could be run without the assistance of an engineer [Aphornratana and Sriveerakul, 2010].

Figure 1.1 Naphtha engine boat (left) and the first ORC working fluid (right).

Today, ORC engines are well–known and widely used, mainly to produce electricity from low–temperature heat sources. They are usually applied with biomass, geothermal, solar thermal, or low–grade industrial waste heat. They are suitable to be used as a bottoming cycle for other internal combustion engines or steam turbine engines. Commercial units with power capacity of 10kW to 1 MW are available. They are operated using R134a or R245fa. The expanders used are radial flow turbine type or screw type. They can be applied when the differential temperature between the heat source and the surrounding is as low as 70°C [Infinity turbine, CALNETIX TECHNOLOGIES, Turboden, Ormat technologies, and EXERGY].

In the ORC system, the expander is a key role component on the system. Each type of expander has its own characteristic which is suitable for each ORC system capacity. Many researchers have developed expanders for with the ORC system. The expanders can be categorized into two types: velocity–type (radial flow expander); and volume–type (scroll expander, piston expander, screw expander, and sliding vane expander).

From the literature [Qiu et al., 2011], it was found that the volume–type expander are more practical for the micro–scale ORC system because they are characterized by lower flow rates, higher pressure ratios, and much lower rotational speeds compared with the velocity–type expander. The volume–type expanders can tolerate two–phase flow conditions, which may appear at the end of expansion in some operating conditions.

The sliding vane expander, which is a volume–type expander, is selected to apply with a micro–scale ORC system. This expander is very attractive in applications

where low initial cost and high power density are much more important than efficiency. Although its efficiency is relatively low compared to the other types, it has relatively simple structure and consists of a comparatively small number of low cost parts [Lord, 1984].

In this study, two sliding vane expanders (2AM and 1AM expanders) were developed for a micro–scale ORC system. They were modified from two commercially available air motors (GAST 2AM and GAST 1AM). The 2AM and 1AM expanders were totally manufactured in–house at the SIIT mechanical engineering laboratory. They were redesigned by keeping the original essential dimensions and operating principles of the original GAST air motors but modified so that the units were leak proof and suitable to use expanders for a micro–scale ORC system. Performance tests were conducted to obtain actual performance and characteristics of these expanders. Two methods of power measurement were employed: Prony brake and electrical power. The effect of operating conditions on the expander performance was investigated.

This thesis consists of five chapters, including this current chapter. In Chapter 2, the background and literature review related to the development of the sliding vane expander is summarized. In Chapter 3, the detail of the design and construction of an ORC experimental rig are presented. In Chapter 4, discussion of the results influenced by the operating conditions is presented. Lastly, Chapter 5 includes general conclusion, discussions and recommendations for future research.

Chapter 2
Background and Literature Review

2.1 Background

The Organic Rankine Cycle (ORC) is similar to the traditional steam Rankine cycle. The operation of ORC is the same as Rankine cycle but a different working fluid is used. The main components of the ORC consist of a vapour generator, turbine (or expander), condenser, and pump. The first ORC engine was invented by Frank Ofeldt in the 1880s. The working fluid used was Naphtha and the engine was used to power a small boat. At that time, the government required a license to run steam engines but did not require one when boiled Naphtha. Therefore, with the use of this Naphtha engine, the boat could be run without the assistance of an engineer [Aphornratana and Sriveerakul, 2010].

Organic Rankine Cycle is a well–known and widely used, mainly to produce electricity from low–temperature heat sources. They are usually applied with biomass, geothermal, solar thermal, or low–grade waste heat. They are suitable to be used as a bottoming cycle for other internal combustion engines or steam turbine engines. Commercial units with power capacity 10 kW–1 MW are available. They are operated using R134a or R245fa (organic fluids commonly used as refrigerants for refrigeration machines). The expanders used are radial flow turbine type or screw type. They can be applied when the differential temperature between the heat source and the surrounding is as low as 70°C. [Infinity turbine, CALNETIX TECHNOLOGIES, Turboden, Ormat technologies, and EXERGY]

2.2 Organic Rankine Cycle

The ORC working principle is similar to the traditional steam Rankine cycle. Its schematic diagram is illustrated in Figure 2.1. Its main components consists of vapour generator, condenser, pump, and turbine (in this study, the turbine will be called an expander). The saturated liquid (1) is heated to saturated vapour (2). The high pressure and temperature saturated vapour (2) is expanded, through the isentropic expander, to a low pressure (3). The low pressure working fluid vapour (3) is then passed through

the condenser where heat is rejected to the surrounding. At the condenser, the working fluid is condensed to liquid (4). The liquid (4) is then pumped isentropically through a mechanical pump prior to entering the vapour generator, and thus completing the cycle.

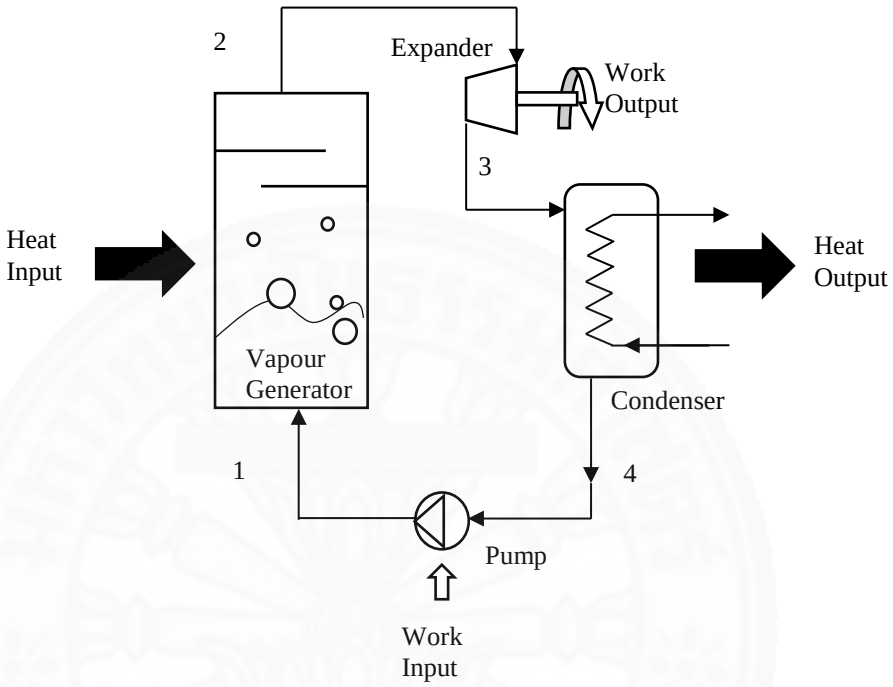

Figure 2.1 Schematic diagram of the ORC system.

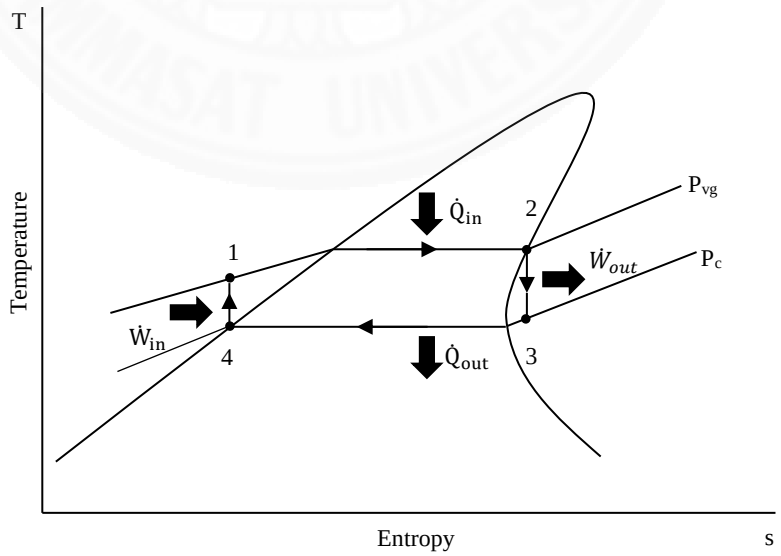

Figure 2.2 T–s diagram of ORC system.

Process 1–2 Constant pressure heat addition to the vapour generator

Evaporating of subcooled liquid (1) to saturated vapour (2) at high pressure in a vapour generator. The heat addition to the vapour generator can be calculated by

$$\dot{Q}_{in} = \dot{m} \cdot (h_2 - h_1) \tag{2.1}$$

Where $\dot{Q}_{in}$ Heat input required via the vapour generator (kW)

$\dot{m}$ Mass flow rate of the fluid through the vapour generator (kg/sec)

h_2 Enthalpy of the fluid (saturated vapour) at the vapour generator exit (kJ/kg)

h_1 Enthalpy of the fluid (subcooled liquid) at the vapour generator inlet (kJ/kg)

Process 2–3 Isentropic expansion at the expander

Saturated vapour (2) expands isentropically through the expander from (2) to (3), causing the shaft work to be produced. The work output from the expander can be calculated by

$$\dot{W}_{out} = \dot{m} \cdot (h_2 - h_3) \tag{2.2}$$

Where $\dot{W}_{out}$ Power produced at the expander (kW)

$\dot{m}$ Mass flow of the fluid through the expander (kg/sec)

h_2 Enthalpy of the fluid (saturated vapour) at the expander inlet (kJ/kg)

h_3 Enthalpy of the fluid (superheated vapour or two phase mixture) at the expander exit (kJ/kg).Since the process is isentropic, the entropy remains constant ($s_2 = s_3$)

Process 3–4 Constant pressure heat rejection at the condenser

Low pressure expander' exhaust (3) is liquefied to saturated liquid (4) by rejecting heat to the surrounding. The condenser pressure (P_{con}) is equal to the saturation pressure at the working fluid temperature (T_4).Heat rejected at the condenser can be calculated by

$$\dot{Q}_{out} = \dot{m} \cdot (h_3 - h_4) \tag{2.3}$$

Where $\dot{Q}_{out}$ Heat rejected at the condenser (kW)

$\dot{m}$ Mass flow rate of the fluid through the condenser (kg/sec)

h_3 Enthalpy of the fluid (superheated vapour or two phase mixture) at the condenser inlet (kJ/kg)

h_4 Enthalpy of the fluid (saturated liquid) at the condenser exit (kJ/kg)

Process 4–1 Isentropic pumping at the pump

Saturated liquid (4) is pumped from the condenser pressure (P_{con}) to the vapour generator pressure (P_{gen}). The power input to the pump can be calculated by

$$\dot{W}_{in} = \dot{m} \cdot \upsilon_1 \cdot (P_1 - P_4) \tag{2.4}$$

Where $\dot{W}_{in}$ Power consumed at the pump (kW)

$\dot{m}$ Mass flow of the fluid through the pump (kg/sec)

υ_1 Specific volume of the fluid (subcooled liquid) at pump exit (m^3/kg)

P_1 Pressure of the fluid (subcooled liquid) at pump exit (kPa)

P_4 Pressure of the fluid (saturated liquid) at the pump inlet (kPa)

Thermal efficiency of an ORC is then calculated by

$$\eta = \frac{\dot{W}_{out} - \dot{W}_{in}}{\dot{Q}_{in}} \tag{2.5}$$

Where η Thermal efficiency of the ORC system

$\dot{W}_{out}$ Power produced via the expander (kW)

$\dot{W}_{in}$ Power consumed via the pump (kW)

$\dot{Q}_{in}$ Heat input required via the vapour generator (kW)

Since $\dot{W}_{in}$ is very small compared to the expander power (usually it is less than 1%), it can be neglected. The efficiency can be simplified as

$$\eta = \frac{\dot{W}_{out}}{\dot{Q}_{in}} \tag{2.6}$$

2.3 Working fluid selection

The system performance of the ORC system depends significantly on the working fluid selection. The rapid development of ORC has encouraged numerous researchers to study the ORC with various working fluids. Many researchers conducted experiments or simulations to prove that performance of the ORC system depends on the working fluid used. The criteria to select the type of the working fluid used for the ORC system should be made as follows:

- It is environmentally friendly
- It is non–flammable and non–toxic
- It is available at low cost or acceptable cost
- It has a reasonable boiling point at atmospheric pressure (so that there is no need for heavy construction)

The working fluid can be categorized by the saturation vapour curve, which is one of the most crucial characteristics of the working fluid in an ORC. There are two general types of vapour saturation curves in the temperature–entropy (T–s) diagram: wet fluid; and dry fluid. For the wet fluid (R134a, R123, R707 (steam), and R710 (ammonia)), the saturated vapour line always provides the negative slope on T–s diagram. It is illustrated in Figure 2.3. When the wet fluid expands through the expander, its state is always on the saturated liquid–vapour mixture which is considered as two phase flow. Two phase fluid travelling through the expander usually provides a negative impact on the expander and expander's performance. It may damage turbine blades, and also reduces the isentropic efficiency of the expander. Typically, the minimum dryness fraction at the outlet of an expander is kept above 85%. To satisfy the minimum dryness fraction at the outlet of the turbine, high pressure vapour at the inlet of the expander should be superheated [Bao and Zhao, 2013].

For the dry fluid, its saturated vapour line provides a positive slope on T–s diagram. It is illustrated in Figure 2.4. As the dry fluid travels through the expander, it can be seen from the curve that the dry fluid is always in the dry vapour phase. This means that dry fluid does not required superheating, thereby eliminating the concerns of impingement of liquid droplets on the turbine blade. Therefore, the working fluids

of “dry” type are more suitable for ORC systems. Examples of dry fluid are R245fa, R1234yf, and R141b.

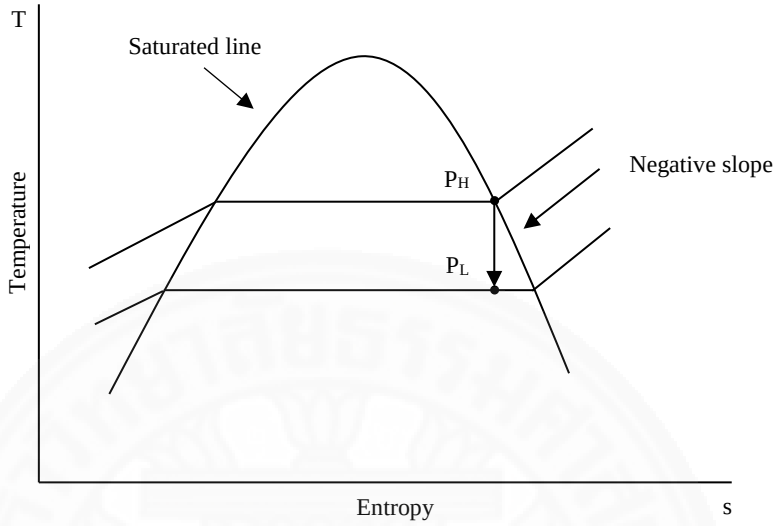

Figure 2.3 Expansion process for wet fluid plotted on T–s diagram representing the negative slope of wet fluid.

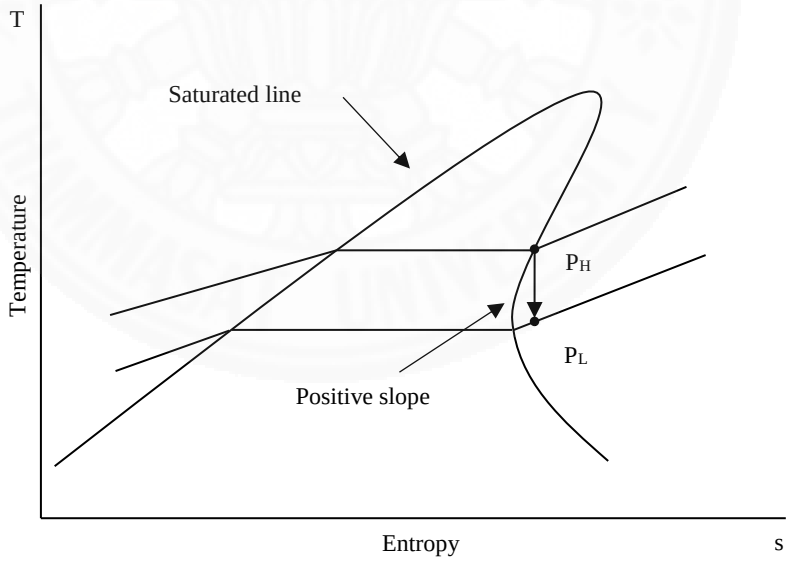

Figure 2.4 Expansion process for dry fluid plotted on T–s diagram representing the positive slope of dry fluid.

R141b, which is a kind of HCFC refrigerant, is considered as one of the dry fluids which provides the positive impact on the expander. It has been selected to be used as the working fluid for this present work. The reason is that R141b is classified as one of the high boiling point organic substances at atmospheric pressure (32.05°C). Therefore, it does not require heavy construction of the vapour generator vessel. Additionally, according to minimum the working pressure within the system is as high as the atmospheric pressure. The problem of leakage of air into the system is easily fixed. It also provides the acceptable performance. Moreover, R141b is readily available at low cost in Thailand. More details of the thermodynamic properties and criteria of selection will be provided in Chapter 3.

2.4 Expander in ORC system

The expander is the key component that significantly affects the ORC performance. Expanders were developed more than a century ago and can be divided into two types: velocity–type (radial flow expander) and volume–type (scroll expander, piston expander, screw expander, and sliding vane expander) [Bao and Zhao, 2013].

The volume–type expanders are more practical for the micro–scale ORC system because they are characterized by lower flow rates, higher pressure ratios, and much lower rotational speeds compared with the velocity–type expander. The volume–type expanders can tolerate two–phase flow conditions, which may appear at the end of expansion in some operating condition [Qiu et al., 2011].

Radial flow expander

A radial flow expander is a type of velocity–type expander. It is the most widely used in ORC systems because it provides the highest isentropic efficiency of the expander compared to the other expanders [Bao and Zhao, 2013]. It also gives a large enthalpy drop between the inlet and outlet with one single stage, due the design of the blade that changes the high velocity of the fluid flow into low speed flow.

Even though the radial flow expander provides highest isentropic efficiency and has a relatively simple structure, it produces a very high rotational speed (15,000–65,000 rpm) when it is applied to the small–scale ORC system [Yamamoto et al., 2001; Nguyen et al., 2001; Yagoub et al., 2006]. Therefore, it needs a reducing gearbox to

reduce its rotational speed to the generator rotational speed [Pei et al., 2011], or a special high speed generator is required [Nguyen et al., 2001; Yagoub et al., 2006; Kang, 2012; Cho et al., 2015]. Moreover, the blade of the expander is difficult to construct which results in a higher cost for construction.

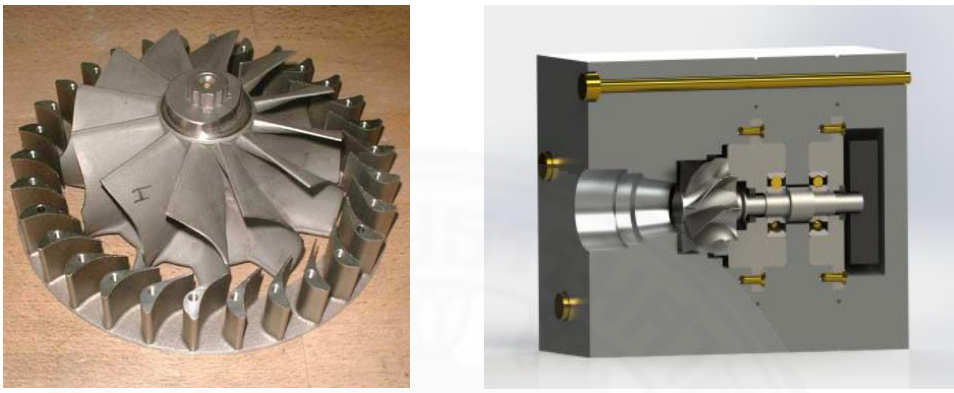

Figure 2.5 Radial flow expander.

Scroll expander

The scroll expander is another widely used expander in small–scale ORC systems. It is a volume–type expander which provides relatively simple operation, low rotational speed, reliability (no valves and few moving parts), and capability to handle high pressure ratios. It is easy modified from a refrigeration compressor [Zanelli and Favrat, 1994] or air compressor [Declaye et al., 2013; Muhammad et al., 2015]. Its structure is a two spiral scroll; one is fixed (stationary scroll) and the other is moving (orbiting scroll). The high pressure working fluid is supplied to the small chamber (formed by the two spiral scroll) at the center of the spiral scroll. As the working fluid expands through the inlet port, it causes the orbiting scroll to move and cause rotational motion. The working fluid expands to the bigger chamber and exits the expander [Lord, 1984].

Although a scroll expander is suitable for a small–scale ORC system, its pressure ratio is fixed by each commercially available compressor. Meanwhile it is necessary to find the appropriate compressor which sometimes is not available in the market. So, the manufacturing of the new expander unit is an alternative way to solve the problem. However, the complicated design of the spiral scroll (stationary and orbiting scroll) makes it difficult to manufacture and construct the expander. This is the

reason why the scroll expander is not preferable to develop for micro–scale ORC system.

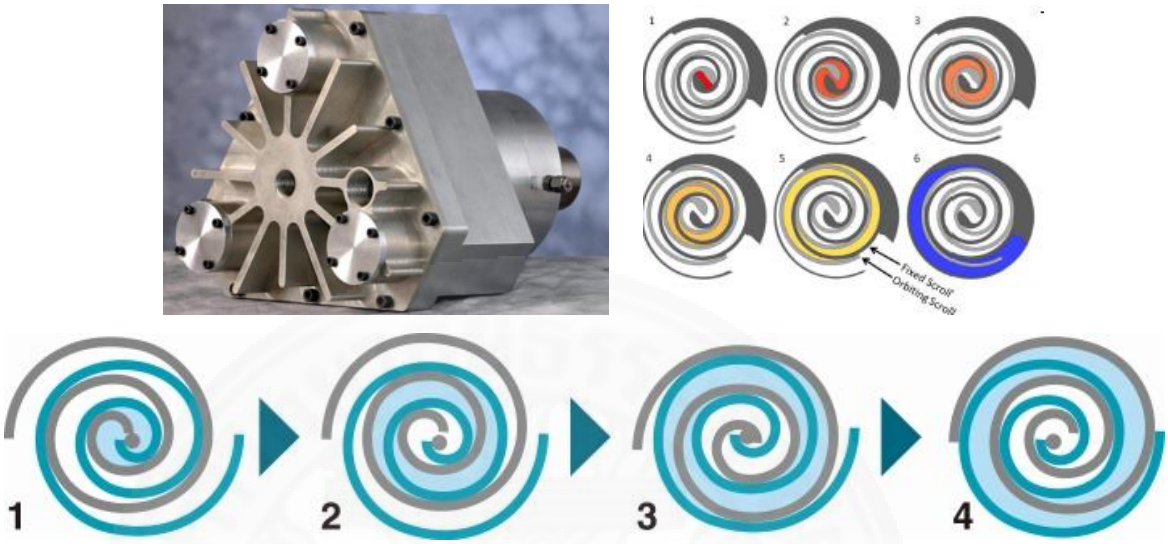

Figure 2.6 Scroll expander.

Piston expander

The piston expander is a volume–type expander. Its working principle is the high pressure vapour working fluid is fed through an inlet valve to a small space enclosed by a cylinder and a piston which is near the end of the cylinder. Then, the inlet valve is closed and the volume is expanded by piston motion away from the end of the cylinder. After the desired expansion has taken place, a discharge valve opens and the working fluid is expelled from the cylinder by piston motion toward the end of the cylinder. Then, the discharge valve closes and the cycle repeats. The piston force is usually converted into torque on the output shaft by a connecting rod and crankshaft mechanism [Lord, 1984].

Even though the piston expander produces a relatively high torque, withstanding high pressure and two–phase working fluid, it is quite complicate to operate. This is because it needs a timing valve control to regulate the inlet and outlet valve. Moreover, many moving parts are used to produce the rotational motion which causes the piston expander to be relatively larger than other expanders with similar working capacities.

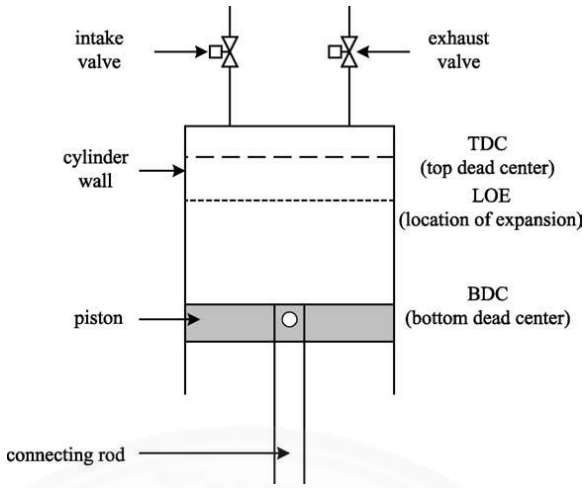

Figure 2.7 Piston Expander.

Screw expander

The screw expander is a volume–type expander. It has two rotors with helical grooves, one male and the other female. The rotors run side by side on parallel shafts so that the grooves mesh with each other, and they are enclosed in a close fitting case. The vapour working fluid enters the machine at one end. As the groove pair continues to disengage, the volume of the working fluid increases, and expansion process takes place. The machine, discharge the fluid at a low pressure at the other end. The working fluid does work on the lobes of each rotor as it expands, and one shaft serves as the power takeoff [Lord, 1984].

Even though the volume–type expander is more appropriate for a micro–scale ORC than the velocity–type, the screw expander is not often used. Most the screw expanders are applied with large systems (more than 30 kW) [Hsu et al., 2014; Smith et al., 2005]. Moreover, the helical rotor is difficult to manufacture making the screw expander less interesting to apply with a micro–scale ORC system.

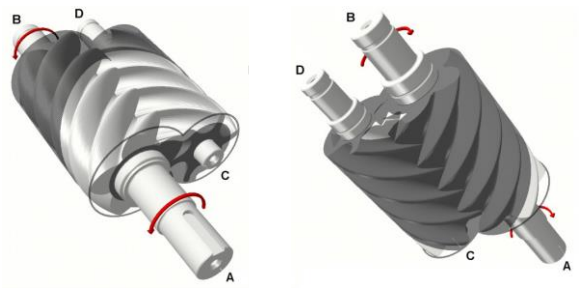

Figure 2.8 Screw expander [Smith et al., 2005].

2.5 Expander for micro–scale ORC system

The radial flow expander and screw expander seem to be a good choice for the large–scale system. The radial type, which is a velocity–type, requires a large amount of fluid flow rate in order to generate the power rather than the pressure ratio. Therefore, for the micro–scale ORC system, the volume–type seems to be more appropriate than the velocity–type.

Even though the screw expander is the volume–type expander, it is usually applied to the large–scale system [Hsu et al., 2014; Smith et al., 2005]. In order to use it in a micro–scale system, the size of its rotors need to be reduced. However, the manufacturing of the helical rotors required a very high precision manufacturing, which will result in a higher construction cost. Moreover, if the rotor is not machined properly, it will become locked easily [Smith et al., 2005]. Therefore, it is not preferable to develop for a micro–scale ORC system.

The operation of the piston expander is quite complicated, due to the timing valve control of the inlet and outlet valve, making this expander unsuitable to use with a micro–scale ORC system.

The scroll expander seems to be the most appropriate expander for a micro–scale ORC system. However, its pressure ratio is usually fixed by the commercially available compressor. Also, it is necessary to find the appropriate compressor which sometimes is not available in the market. The manufacturing of a new expander is an alternative way to solve the problem but the complicated of design of the spiral scroll (stationary and orbiting scroll) makes construction difficult. This is the reason why the scroll expander is not preferable to develop for micro–scale ORC system.

As stated above, there is another type of the volume–type expander that is suitable for the micro–scale ORC system. It is a sliding vane expander and it is extensively used in gas compressors and expanders. However, its main use today is in hand–held pneumatic tools, such as an air motor. A schematic of the concept in an expander configuration is shown in Figure 2.9. The designed concept has a cylindrical rotor running inside an offset cylindrical case. A vane extends from a vane slot in the rotor to the case, to form a chamber [Lord, 1984]. A typical working mechanism of the sliding vane expander is presented as follow:

- At section (1), a chamber is exposed to the inlet port when the volume of the chamber is small.
- As the rotor rotates in section (2), the volume of the chamber is increased, and the expansion takes place.
- After the point where the chamber reaches its maximum volume in section (3), the discharge ports are exposed. The working fluid is then discharged as the chamber volume is decreased in section (3) and (4).

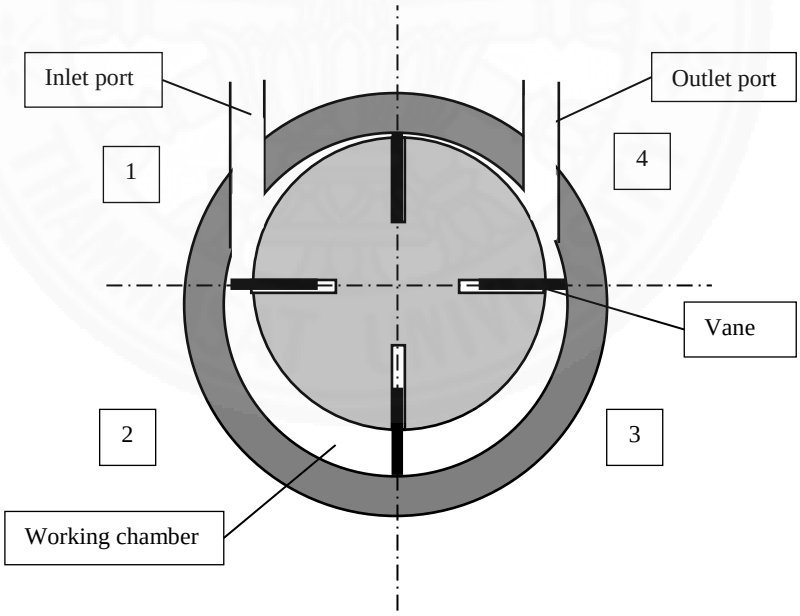

Figure 2.9 Schematic diagram of sliding vane expander.

Figure 2.10 Sliding vane expander.

The sliding vane expander is very attractive in applications where low initial cost and high power density are much more important than efficiency. Although its efficiency is relatively low compared to the other types, it has a simple structure and consists of a comparatively small number of low cost parts [Lord, 1984]. From all of the above reasons, “an air motor”, which is a type of sliding vane expander which is commercially available in the local market, is modified and used as an expander for an experimental micro–scale ORC system by many researchers. The details of the expander development will be provided in Chapter 3.

2.6 Past researches on ORC systems

ORC systems were developed more than a century ago for producing electrical energy and doing mechanical work. Their cycle efficiency relies heavily on the expander and its working conditions. Therefore, most of the current researches concentrate on the improvement of an expander. Many researchers have developed the expander in an attempt to improve the expander’s efficiency. Some studies showed that each type of expander requires a suitable range of the working condition and capacity. In order to achieve the best possible performance for a specified condition, the selection of suitable expander is the first consideration. The summary of the published work is shown in Table 2.1.

Yamamoto et al. [2001], Nguyen et al. [2001], Pei et al. [2011], and Yagoub et al. [2006] have developed the radial flow expander for the ORC system. Their tests were conducted at various working conditions. Usually, this type of expander is applied

to a large–scale system in the commercial unit. However, for a lab–scale the system capacity is not as large as the commercial–scale. It can be seen that the efficiency is not as high as the commercial unit; however, it provides an acceptable efficiency. The thermal efficiency of more than 4% was found [Nguyen et al., 2001; Pei et al., 2011; Yagoub et al., 2006]. For the system capacity below 1 kW, it can be seen that the efficiency drops to be less than 1.5% [Yamamoto et al., 2001]. The expander rotational speed was beyond 10,000 rpm. Therefore, a reducing gearbox or the high speed generator was needed in order to generate useful electrical energy. To optimize the expander efficiency, inlet guide vanes may be equipped in order to guide the working fluid to hit the turbine blade at its best direction, [Yamamoto et al., 2001; Kang, 2012].

Zanelli and Favrat [1994], Peterson et al. [2008], and Declaye et al. [2013] developed the scroll expander for an ORC system. It is modified from a commercially available refrigeration or air compressor. At the system capacity around 1 kW, the thermal efficiency of the system is more than 5% with the moderate rotational speed (≈3,000 rpm).

Hsu et al. [2014], and Smith et al. [2005] developed a screw expander for an ORC system. This type of expander shows the highest thermal efficiency (10.5%) compared to other types. This type of expander is usually applied to the system with a capacity beyond 30 kW. From the literature survey, it is found that this type of expander is rarely developed for the system below 1 kW. This is because of the difficulty of construction of the helical rotor.

Baek et al. [2005] developed the piston expander to replace the expansion valve in the CO_2 refrigeration cycle. It was found that, the piston expander was difficult to operate and involved a complicated working mechanism. Zheng et al. [2013] has developed a rolling piston expander for ORC system. A rolling piston expander is less complicated than a cylindrical piston expander. Even though the mechanical part has been reduced, the timing valve control of the inlet and outlet still need to be used in order to get the rotational motion.

Yang et al. [2009] studied internal leakage in the sliding vane expander which was used to replace the throttling valve in the CO_2 refrigeration cycle. From the study, it was found that the reduction of internal leakage results in an increase of the expander efficiency. Qiu et al. [2012] developed the sliding vane expander for ORC system. The

air motor was modified to use as an expander. The leakage of the organic working fluid was eliminated. The thermal efficiency achieved from the system is around 1.41%. Only a few studies of sliding vane expanders in an ORC system have been conducted.

Table 2.1 The summary of the published work.

	Expander	Working fluid	Power output	Rotational Speed	Thermal Efficiency
Yamamoto et al., 2001	Radial flow expander	R123 Water	150 W 17,000 rpm 150 W 20,000 rpm	>10,000 rpm	≈1.25% <1%
Nguyen et al., 2001	Radial flow expander	n–pentane	1.44 kW 65,000 rpm	>10,000 rpm	≈4.3%
Pei et al., 2011	Radial flow expander	R123	1.36 kW 24,000 rpm (20:1 gearbox)	>10,000 rpm	6.8%
Yagoub et al., 2006	Radial flow expander	n–pentane HFE–301	1.5 kW 60,000 rpm	>10,000 rpm	5% 7.6%
Kang et al., 2012	Radial flow expander	R245fa	32.5 kW	>10,000 rpm	5.22%
Zanelli and Favrat, 1994	Scroll expander	R134a	1 to 3.5 kW 2,400 to 3,600 rpm	<4,000 rpm	1.6 to 5.8%
Peterson et al., 2008	Scroll expander	R123	187 to 256 W 1,053 to 1,287 rpm	<1,500 rpm	7.2%
Declaye et al., 2013	Scroll expander	R245fa	2 kW 3,500 rpm	<4,000 rpm	8.54%
Hsu et al., 2014	Screw expander	R245fa	50 kW 3,610 to 3,670 rpm	~3,600 rpm	10.5%
Smith et al., 2005	Screw expander	R113 R134a Isobutane	>500 kW	–	–
Baek et al., 2005	Piston expander	CO_2	24.35 to 36.53 W 114 to 120 rpm	<120 rpm	–
Zheng et al., 2013	Piston expander	R245fa	350 W 350 to 800 rpm	<1,000 rpm	5%
Yang et al., 2009	Sliding vane expander	CO_2		< 800 rpm	
Qiu et al., 2012	Sliding vane expander	HFE 7000	821.8 to 860.7 W 841 to 860 rpm	<1,000 rpm	1.41%

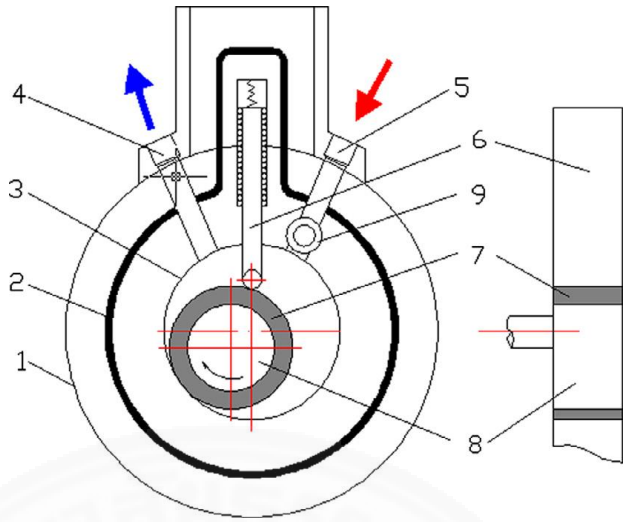

Figure 2.11 A rolling piston expander [Zheng et al., 2013].

Regarding the existing works, the radial flow expander and scroll expander are the most extensively used in ORC systems. Even though the radial flow expander provides the highest isentropic efficiency and has a relatively simple structure, it produces very high rotational speed (more than 10,000 rpm). Therefore, it requires an external reduction gearbox or a special high speed generator [Pei et al., 2011; Nguyen et al. 2001; Yagoub et al., 2006; Pei et al., 2011; Kang, 2012; Cho et al., 2015]. For the scroll expander, it is convenient to use with the ORC system by easily connecting the conventional compressor in the backward direction with a slight modification to prevent the leakage of the working fluid. However, the structure designed especially in the stationary scroll and orbiting scroll is quite complicate for the further modification [Zanelli and Favrat, 1994; Declaye et al., 2013; Muhammad et al., 2015].

2.7 Conclusion

Using an ORC system is recognized as a promising way to produce useful mechanical work which is consistent with the current energy and environmental situation. This is used to utilize the low–grade heat which is mostly considered as waste.

There are various types of expander which can be used in an ORC system, including piston expander, screw expander, and sliding vane expander. Piston expander might be rarely used due to the complexity of the inlet and outlet valve timing control. The screw expander requires a very high precision of manufacturing process. Therefore,

these two types of expanders are not a good choice for the micro–scale ORC system (less than 10kW). The sliding vane expander is another type of expander which is relatively simple to design, construct, and operate. Hence, the construction cost is the cheapest compared to the other expanders. Although its efficiency is relatively low compared to other types, it is recognized as the most promising option due to its simplicity of structure and construction. However, only a few researches have focused on the development of the sliding vane expander to apply with the ORC system.

From the literature survey, most of the published work was conducted based on experimentation with the variation of time. There is a lack of the published works which demonstrates the expander performance. Therefore, a comprehensive test to examine the expander performance is needed. The understanding of the key performance indicator of each type of expander is made possible. Even though the evidence of the practical use is available [Yamamoto et al., 2001], it does not give the knowledge concerned with the expander development. This means a more comprehensive test to demonstrate the expander performance is necessary to make further progress in this research field. This present work is aimed to comprehensively investigate the sliding vane expander.

Chapter 3
Experimental Organic Rankine Cycle (ORC) rig

In this chapter, the details of the ORC experimental rig are explained. It was designed and constructed to demonstrate the performance of the small sliding vane expanders. Working fluid used was R141b. The details of the development of the sliding vane expanders are also provided.

3.1 Working fluid selection

The system performance of the ORC system depends significantly on the working fluid selection. The criteria to select the type of the working fluid used for the ORC system should be made as follows:

- It is environmentally friendly
- It is non-flammable and non-toxic
- It is available at low cost or acceptable cost
- It has a reasonable boiling point at atmosphere so that there is no need for heavy construction of the system component
- The boiling point should not be higher than the ambient temperature. Therefore the condenser pressure is not below the atmospheric pressure. This eliminate the problem of air leakage into the system.

The working fluid can be categorized by the saturation vapour curve, which is one of the most crucial characteristics of the working fluid in an ORC. There are two general types of vapour saturation curves in the temperature–entropy (T–s) diagram: wet fluid and dry fluid. In the case of using wet fluid, the liquid droplet might occur at the end of expansion process which may result in damage to the expander blade. To avoid that problem, it would be better to use dry fluid.

In this study, R141b (Dichlorofluoroethane, $CC_{12}F–CH_3$), which is dry fluid, was used as a working fluid for the performance testing of the sliding vane expander. R141b was used because it is a low pressure working fluid, it provides acceptable performance, it is nontoxic and nonflammable, it has reasonable global warming

potential (GWP) and ozone depletion potential (ODP), and it is easily available at low cost in local market. R141b has a high boiling point (32.05°C) but still is lower than water. The advantage of using a high boiling point working fluid is that it remains in liquid phase at room conditions (it can be put in an open container). Therefore, it is easy to handle.

The experimental system was designed so that can be modified or disassembled with little loss of R141b. The vapour generator pressure is at modulated pressure, so there is no need for heavy construction. At the condenser, the pressure is approximately the same as the atmospheric value. Table 3.1 shows the physical properties table of R141b

Table 3.1 Physical property table for R141b

Physical properties	**R141b**
Molecular weight	116.95
Boiling point at atmosphere (°C)	32.05
Density of liquid at 25°C (g/cm^3)	1.227
Vapour pressure at 25°C (MPa)	0.079
Critical temperature (°C)	204.15
Critical pressure (MPa)	4.25
Critical density (g/cm^3)	0.430
Latent heat of vaporization at boiling point (J/kg)	223.0
Solubility in water at 25°C (% by weight)	0.509
Specific heat, liquid at 25°C (kJ/kg°C)	1.16

3.2 ORC experimental rig

Figure 3.1 shows the schematic diagram of the ORC experimental rig. It is designed and constructed to study and demonstrate the actual performance of the sliding vane expander ORC system. The experimental rig consists of a vapour generator, an expander, a condenser, a receiver tank, and a circulating pump.

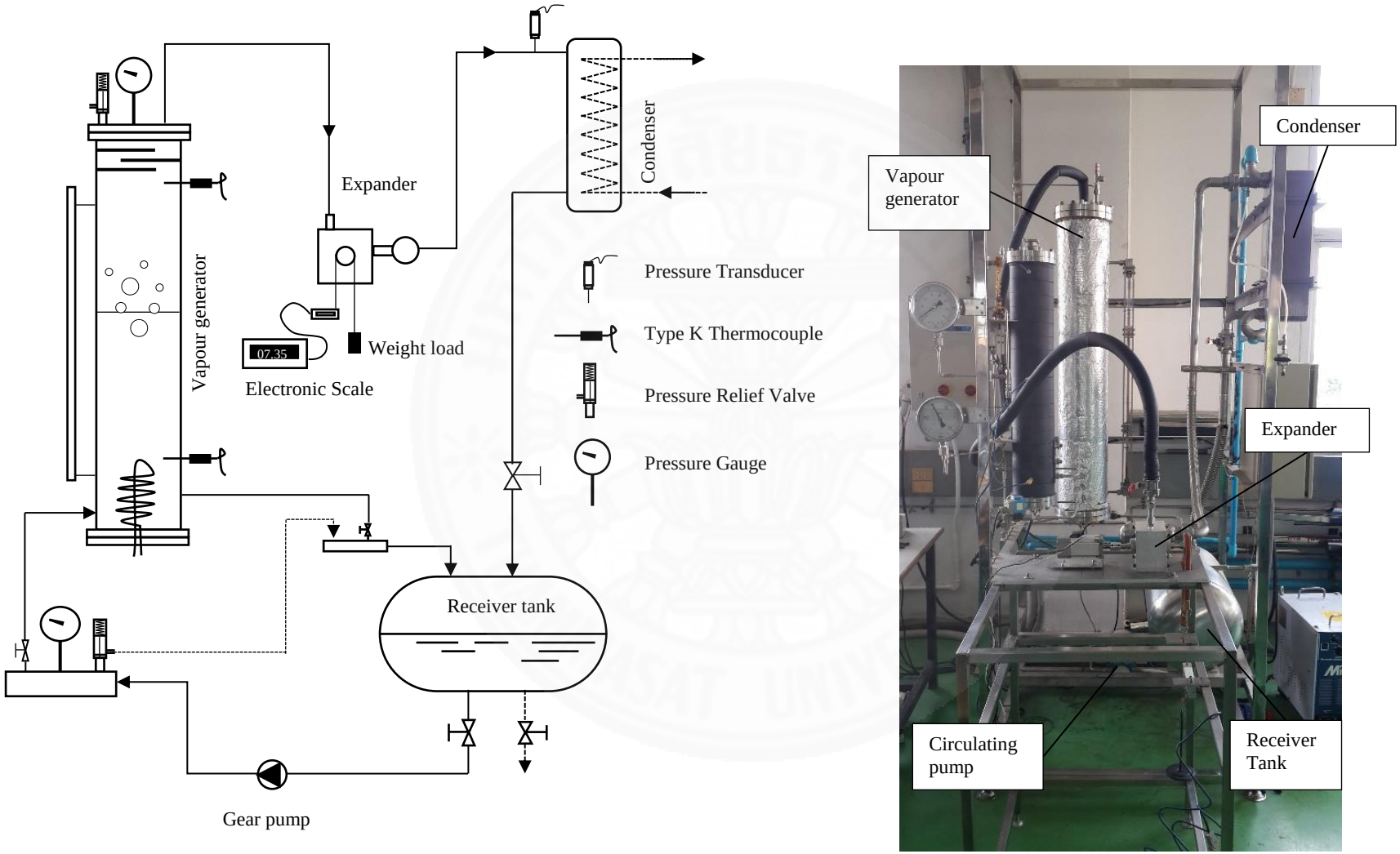

Figure 3.1 ORC experimental rig.

3.2.1 Vapour generator

The vapour generator was made from 6–inch 304 stainless steel pipe schedule 40s (ID = 128.2 mm and OD = 141.3 mm) with a length of 120 cm. Stainless steel flanges were welded to the top and the bottom. A teflon–joint gasket was used as a sealing material. At the top of the vapour generator, three stainless steel baffles were installed to prevent the liquid droplets from being carried over with the vapour. A pressure relief valve with setting pressure of 15 bar was installed at the top flange. The outer surface of the vapour generator was insulated with aluminum foil baking–glass fiber wool. A heat load supply of up to 15 kW was generated by 3 sets of immersion electric heaters located at the bottom flange.

The liquid level inside the vapour generator could be observed by an attached sight glass. The saturation temperature of the working fluid was regulated precisely by a PID temperature controller (Shinko model JSC–220). Since the R141b, a dry fluid type, was used as a working fluid, the super heater was not required which means the working fluid produce by the vapour generator was always in the dry saturated vapour phase.

The temperature at points of consideration was measured by type–K thermocouple probes. The pressure inside the vapour generator was detected by Bourdon pressure gauge (WIKA) –1 to 25 bar and the pressure transducer with an uncertainty of ±1.0% of full scale (DIXELL, PF11a).

3.2.2 Condenser and receiver tank

The condenser was a water cooled plate heat exchanger manufactured by SWEP (model CBE–B80Hx64/1P–SC–M). Its total heat transferring area was approximately 2.45 m^2. The cooling water was provided by a vapour–compression chiller. The advantage of using a water chiller rather than using a conventional cooling tower is the temperature of the cooling water can be adjustable precisely and independent from the ambient condition. Saturation pressure within the condenser, which is recognized as the expander's exit pressure, was controlled by adjusting the flow rate of the cooling water. An on–off solenoid valve was used to manage the cooling water flow rate passing through the condenser. A pressure transducer, DIXELL model PF11a, was used to monitor the saturation pressure at the condenser.

The low pressure working fluid vapour is liquefied within the condenser and then flow down to a receiver tank by gravitational force. The receiver tank was designed based on capsule ends cylinder shape. It was fabricated from stainless steel 304 with diameter of 320 mm and length of 550 mm. Both ends were welded with the half spherical caps. The receiver tank was placed at the bottom of the system in order to collect the working fluid from the vapour generator (if it needed to be empty). A sight glass was attached at the side of the tank in order to observe the level of the liquid.

3.2.3 Feed Pump

To feed the liquefied working fluid from the receiver tank back to the vapour generator, the mechanical gear pump, which is a promising choice for use as a feed pump, was used. Since the gear pump is one of the positive displacement pumps which has no inlet check valve, the pressure drop at the suction port is minimized. As a result, the cavitation at the pump's suction is relieved. This is due to the fact that the liquid refrigerant (organic substance) at the suction line is usually in the saturated condition, and therefore, with a slight pressure drop in the suction line, the cavitation will always occur.

An electrically driven gear pump, National refrigeration product model LP22, was used as the working fluid feed pump. It was driven by 1/2 hp–220 VAC motor. The feed pump unit is shown in Figure 3.2. With the use of this pump unit, the maximum flow rate up to 4 liters/min could be made while its differential pressure was up to 20 bar. The small pressure gauge was also installed to observe the discharge pressure. In addition, a pressure relief valve was used to limit pressure at the discharge line for system protection. In such a case, as the pressure of the discharge line is higher than the limited value, the working fluid within the discharge line will be bypassed into the receiver tank in order to reduce the pressure of the discharge line.

Figure 3.2 Feed pump unit.

3.3 Sliding Vane Expander

A sliding vane expander is a volume–type (or positive displacement type). It consists of a body, a rotor, and set of blades. A circular chamber is bored at the center of the body. The rotor of a smaller diameter is placed inside the chamber as shown in Figure 3.3. The center of the rotor is placed eccentrically to that of the chamber so that the outer wall of the rotor makes contact with the inner wall of the chamber at one point. Two or more sliding vanes are equipped with the rotors. When the rotor rotates, volume of the chamber formed between two vanes will be varied as shown

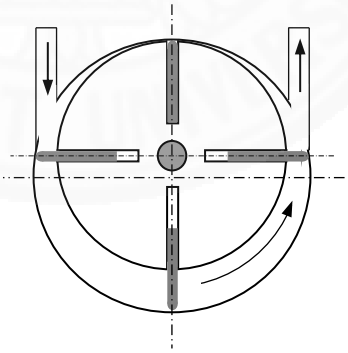

Figure 3.3 Sliding vane expander.

Figure 3.4 shows the working mechanism of a sliding vane expander. It can be seen that the high pressure fluid vapour enters the expander at the inlet port at section (1). It hits the expander's vane causing the rotational motion of the rotor. As the rotor rotates from section (1) to section (2), the volume of the working chamber increases,

and the expansion process take place. After the point where the chamber reaches its maximum volume in section (3), the chamber volume decreases in section (3) and (4), and the fluid vapour is discharged out from the expander.

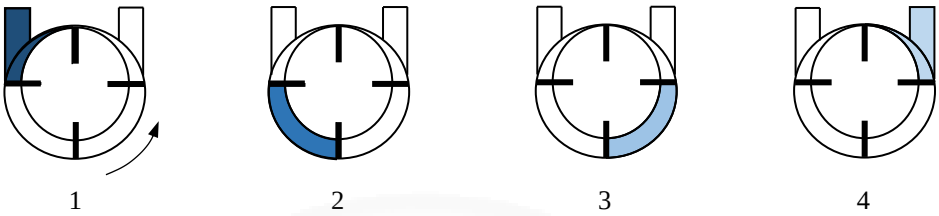

Figure 3.4 Working mechanism of the sliding vane expander.

In this study, two different designs of sliding vane expanders were designed, manufactured, and tested with the experimental ORC rig. They were designed based on sliding vane type air motors which are available commercially in the local market. The air motors were not originally designed to be used with other types of working fluid than air; therefore, they are not designed to be used with a completely closed system in which the leakage of the working fluid is prohibited.

A GAST 2AM air motor and a GAST 1AM air motor were selected and purchased. These two types of air motor were selected because they provide a reasonable power output compared to other air motors which are available locally. The GAST 1AM air motor provides less shaft power output, but at a rotational speed of 10,000 rpm. The GAST 2AM air motor provides more power at a reasonable rotational speed of 3,000 rpm.

Table 3.2 Specification of the GAST 1AM and GAST 2AM air motors.

	GAST 1AM	GAST 2AM
Maximum rotational speed	10,000 rpm	3,000 rpm
Maximum power output	0.33 kW (0.45 hp)	0.68 kW (0.93 hp)
Free air consumption	20.5 CFM	30 CFM

Before the final version of 2AM and 1AM expanders were successfully developed and manufactured, three versions of the air motors and expanders were used. They are:

- GAST 2AM and 1AM air motors are the original units directly from the local supplier.
- Modified GAST 2AM and 1AM air motors are the modified units of the original air motors. O-ring grooves and shaft seals are applied to the original GAST air motors in order to achieved totally leak proof units.
- 2AM and 1AM expanders are the totally redesigned and in–house manufactured units. These are the expanders that actually were used in this study.

3.3.1 Development of 2AM expander

GAST 2AM air motor

To efficiently modify the air motor, it is first necessary to understand the working principle of the air motor. This air motor consists of body, covers, rotor and shaft, and vanes which are shown in Figure 3.5. The working principle can be explained by Figure 3.6 as follows:

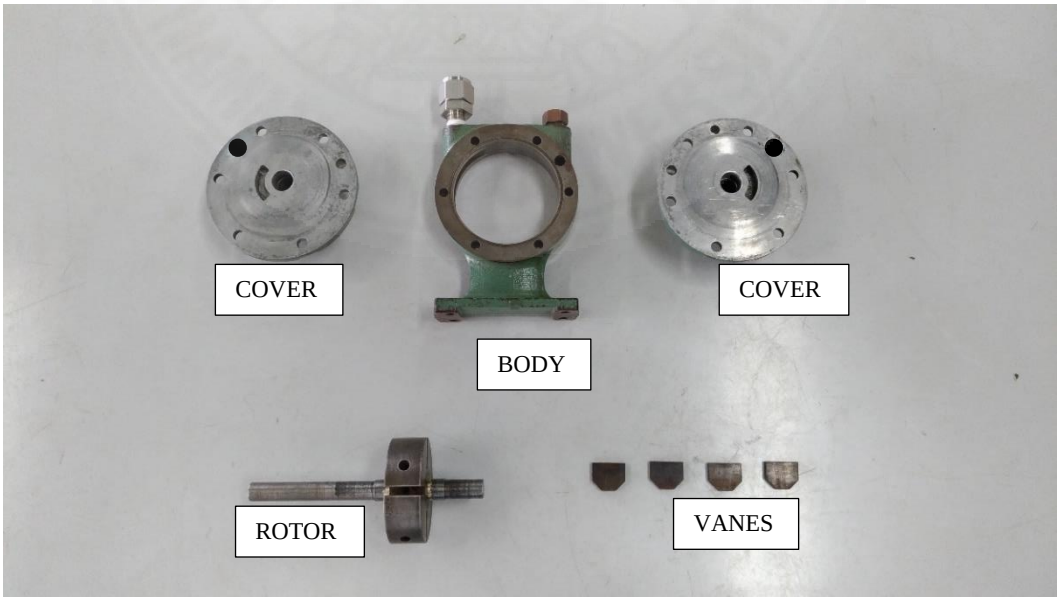

Figure 3.5 Components of GAST 2AM air motor.

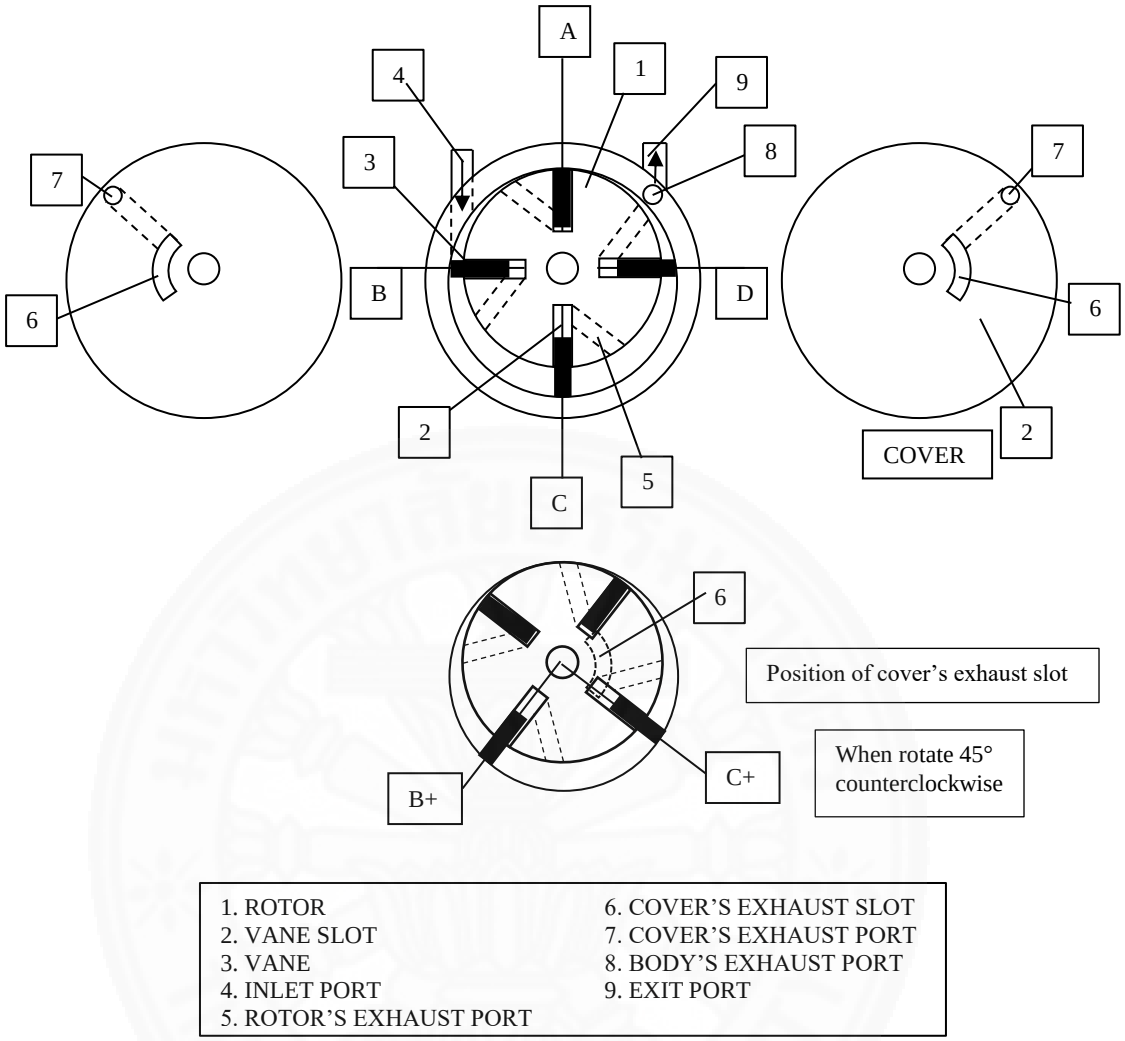

Figure 3.6 Components of GAST 2AM air motor.

The compressed air enters the air motor via the inlet port (4). The air pushes the blade (3B) to rotate in counterclockwise direction. As the rotor rotates, it can be seen that volume of the air expands and increases (from the figure, chamber formed between 3B–3C is larger than that between 3A–3B). The expansion takes place when the rotor rotates from 3A to 3C+. It can be imagined that the chamber formed between 3B+ and 3C+ has the largest volume. Therefore, the air is fully expanded when the vane reaches position 3C+.

After the air is fully expanded (the vane is at position 3C+) and the rotor is further rotated, the bottom of the vane slot 2C+ is opened to the cover's exhaust slot (6). This allows the fully expanded air to be released from the chamber. The air is released out via the rotor's exhaust port, which is a hole drilled from the rotor outer edge to the bottom of the vane slot (5), and comes out from the rotor at the bottom of the vane slot. Then, the air from the rotor enters the cover's exhaust slot (6) and comes out from cover at the cover's exhaust port (7). The exhaust air from both covers come together at the body exhaust's port (8) and are discharged out to the surrounding via the exit port (9).

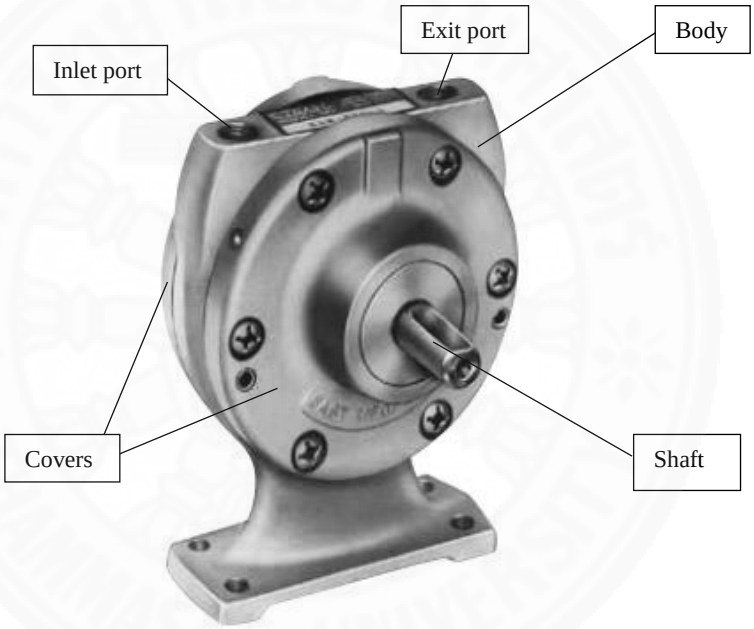

Figure 3.7 GAST 2AM air motor.

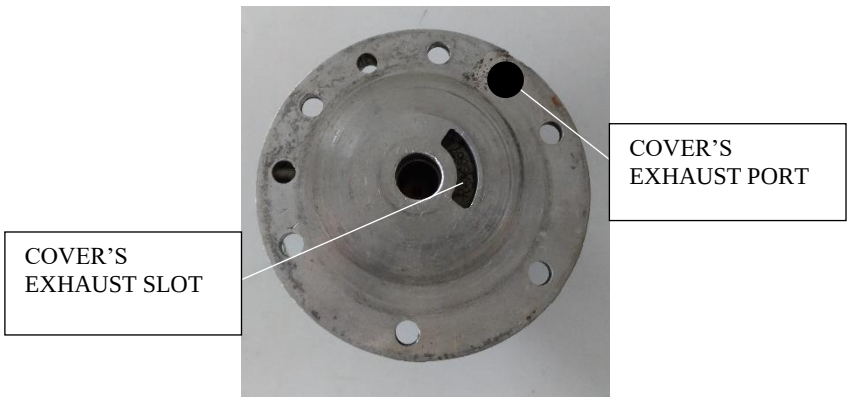

Figure 3.8 2AM air motor cover.

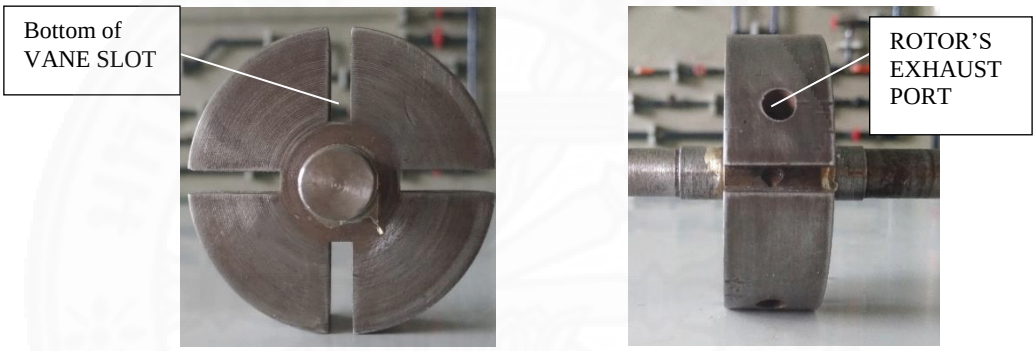

Figure 3.9 2AM air motor rotor and shaft.

Modification of GAST 2AM air motor

To use a commercial air motor as an expander for the ORC system, the elimination of the working fluid leakage is a major issue. This is because the air motor is not designed to work with other types of working fluid, whereas some leakage of air is acceptable. In the case of using organic fluid, in which leakage is prohibited, the GAST 2AM air motor was developed in two steps: 1) the modified GAST 2AM air motor; and 2) the totally in–house manufactured 2AM expander.

The original GAST 2AM air motor was modified to ensure that the leak proof unit was obtained. The air motor is usually designed to use air as the working fluid and the leakage of air is acceptable. To prevent the leakage of the working fluid, O-rings and shaft seals were applied. Nitrile Butadiene Rubber (NBR) Shaft seals were used to prevent the leakage at the shaft. The PTFE and Viton O-rings were used to prevent the leakage between the covers and the body. The reason for using PTFE and Viton was it

could tolerate the heat and corrosive nature of the working fluid. For the shaft seal, NBR was the only material that was available in the local market. Although it could not withstand the heat and corrosion from the working fluid as well as PTFE or Viton, the frequent replacement of the shaft seal was the solution.

Figure 3.10 shows the modified GAST 2AM air motor. A grove for the O-ring was machined on the body of the GAST 2AM air motor. However, it can be seen from the figure that it was not possible to machine the O-ring groove for the body exhaust port (drilled on the body). Thus, a totally sealed GAST 2AM was not possible. To solve this problem, it was decided to drill an exit port on each cover. The exhaust exiting from these two ports were discharged directly to the condenser as shown in Figure 3.11.

Figure 3.10 Modified GAST 2AM air motor with PTFE and Viton O-rings.

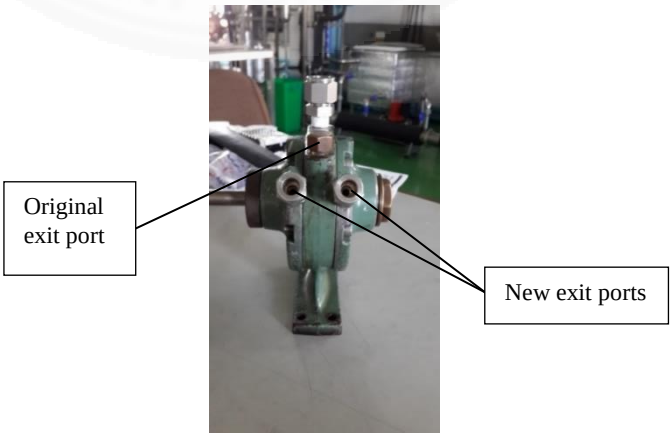

Figure 3.11 Modified GAST 2AM air motor with new exit ports.

To make sure that the modified GAST 2AM air motor was workable throughout the design condition, a test was conducted. To implement this test, the high pressure vapour of R141b at 90°C was supplied to the modified GAST 2AM air motor. It was found that the modified air motor performance was very poor. Even when higher pressure working fluid was supplied, the shaft speed was still below the design value (there was no load applied). However, when the supplied high pressure vapour was reduced, by partially closing the ball valve connected between the vapour generator and the modified air motor, the modified air motor performed better. The shaft rotational speed increased. It is believed that the exhaust vapour was choked at the exit ports. To prove this assumption, the exit ports of the modified air motor were temporally opened to the atmosphere. It was found that the expander performed much better and the shaft rotational speed increased dramatically. It could be concluded that the choked flow was occuring at the exit ports.

To fix this choked flow problem, the flow area at the exit ports had be enlarged. However, this could not be done on the modified GAST 2AM air motor. The thickness of both covers, where the exit ports were drilled, was only 8 mm. Therefore the diameter of the exit port could not be larger than 4.5 mm. It was concluded that the modified GAST 2 AM air motor could not be further modified. It was decided to redesign and totally manufacture a completely new expander unit.

2AM expander

As mentioned earlier, the new expander must be manufactured for the reasons stated above. This section provides the details of the 2AM expander. The picture of the 2AM expander is shown in Figure 3.12. Most of the geometries are identical to the GAST 2AM air motor except for the size of the exhaust system. All the exhaust ports (at the rotor, at the covers, and at the body) were enlarged to prevent the choked flow that might occur in the exhaust ports. The body and two covers were machined from aluminum alloy. The rotor, the shaft, and two bearing holders were machined from stainless steel. The vanes or blades were machined from Bakelite. Bakelite is a material that has low friction which is suitable for sliding work in the expander.

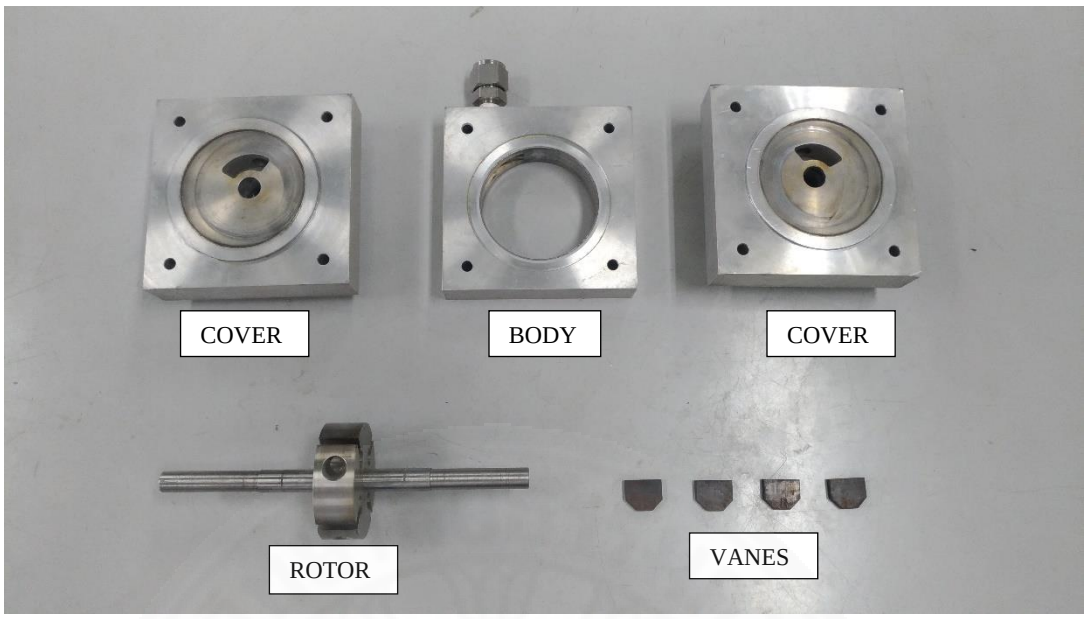

(a) 2AM expander components

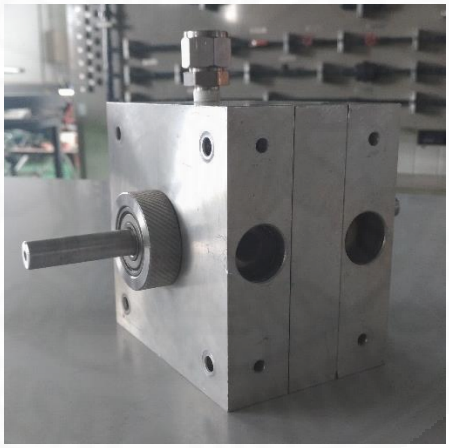

(b) 2AM expander

Figure 3.12 2AM expander.

At the exit ports, the discharged diameter has been enlarged from 4.5 mm (for the modified GAST 2AM air motor) to 18 mm as shown in Figure 3.13. This increased the exhaust flow area by 16 times. This was possible since the covers of the newly design unit were as thick as 30 mm (compared with 8 mm for the original GAST 2AM air motor). The thread fitting was replaced with a straight pipe with O-rings as shown in Figure 3.14. Moreover, the width of the cover's exhaust slots at the covers were enlarged from 6.5 mm to 10 mm as shown in Figure 3.15. Therefore, it was ensured that, the problem associated with the exhaust choked flow was completely eliminated.

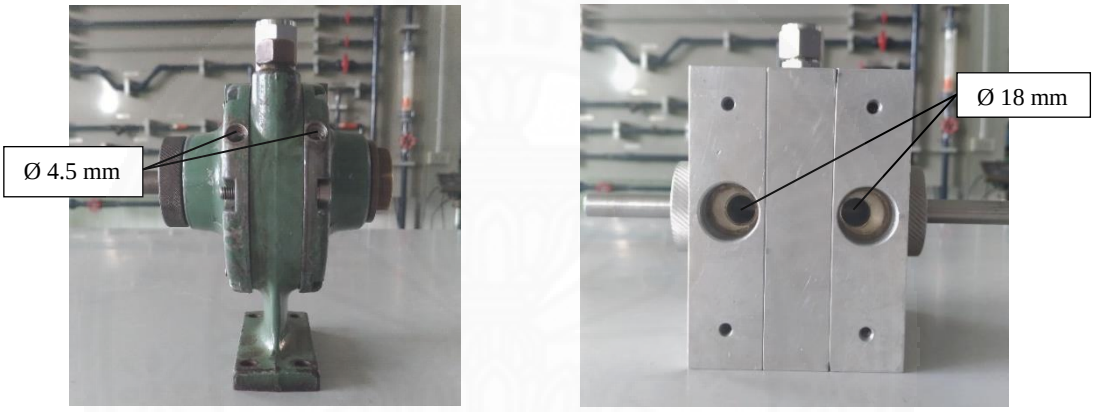

Figure 3.13 Dischage diameter of the expander.

Figure 3.14 Straight pipe with O-rings.

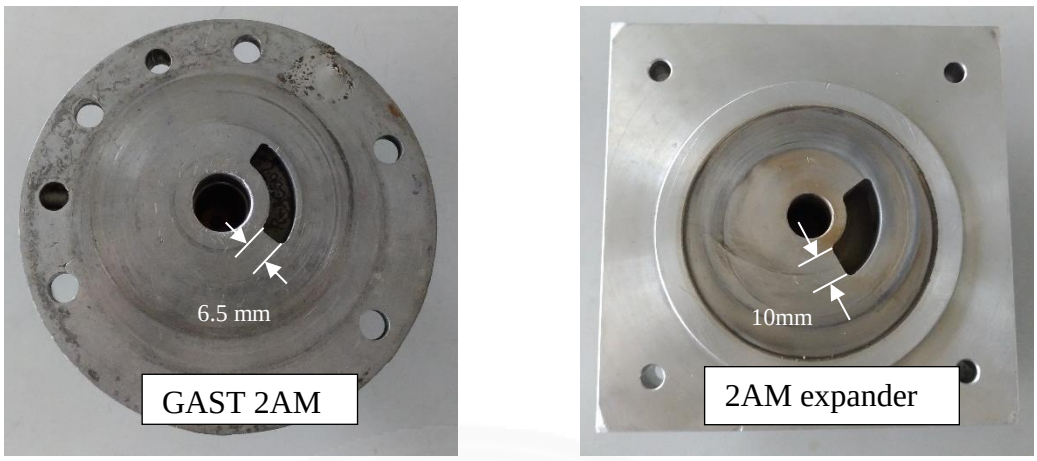

Figure 3.15 Cover's exhaust slots of the expander.

The rotor, which was machined from stainless steel, is very similar to that of the original GAST 2AM unit. However, the rotor's exhaust port was enlarged from 6.5 to 10 mm as shown in Figure 3.16. At the bottom of the vane slot, a 10mm hole was drilled to enlarge the working fluid flow area as shown in Figure 3.16.

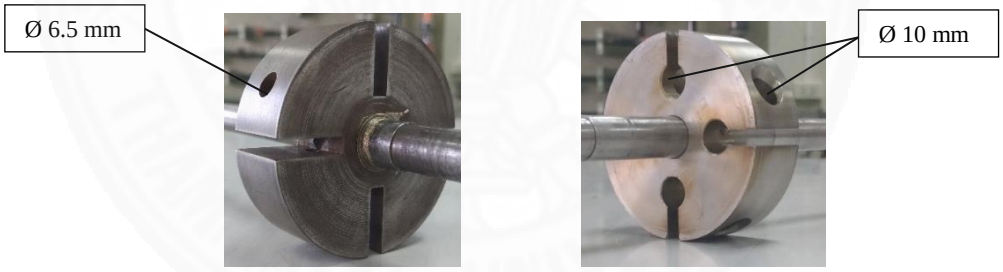

Figure 3.16 Original rotor (left) and Stainless steel rotor (right).

For maintenance purposes, the bearing and shaft seal holders were constructed as shown in Figure 3.17. So the bearing and shaft seal could be easily replaced. In the original GAST 2AM the bearing made direct contact with the working fluid which caused the lubrication oil to be washed out. To solve this problem for the 2AM expander, the bearing was placed at the outside of the bearing and oil seal holder. The geometry drawing of the 2AM expander is provided in Appendix A.

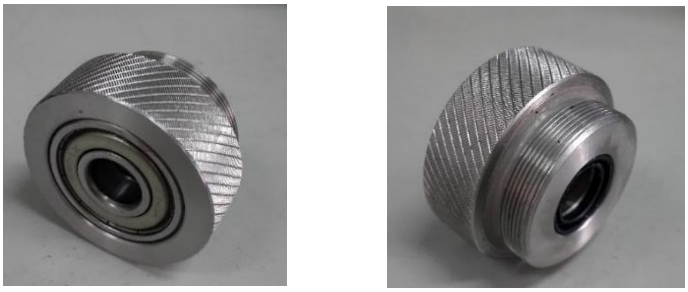

Figure 3.17 Bearing and Shaft seal holder.

3.3.2 Development of 1AM expander

GAST 1AM air motor

The GAST 1AM air motor is a small version of the GAST 2AM air motor. It produces 50% less shaft power output than its bigger brother, the GAST 2AM air motor. However, the shaft speed is 3 times higher, around 10,000 rpm. While the design is much simpler, the operation is exactly the same as described in section 3.3. It consists of a body, two covers, a rotor and shaft, two guide rings, and four vanes which are shown in Figure 3.18. Two guide rings on the rotor are equipped to ensure that the four vanes always slide out from the vane slot without the need of centrifugal force.

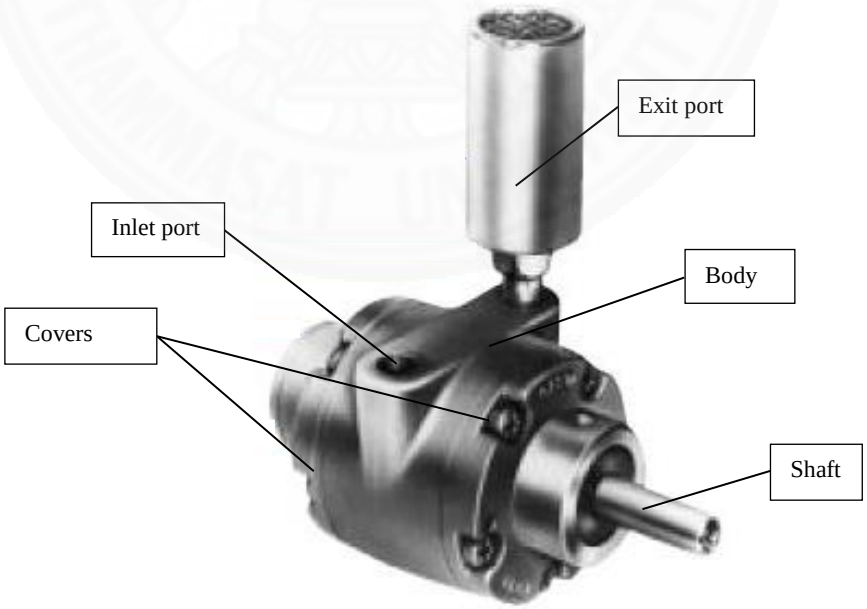

Figure 3.18 GAST 1AM air motor.

1AM expander

For reasons similar to the 2AM expander, it is not easy to modify the original commercial air motor and use it as the expander for the ORC system. Thus, it was decided to design and manufacture a completely new unit of the 1AM expander. The important geometries of the 1AM expander are very similar to those of the GAST 1AM air motor. The picture of the 1AM expander is shown in Figure 3.19.

Similar to the 2AM expander, the body, the covers, the rotor, the shaft, the vanes, and the guide rings were machined from aluminum alloy, stainless steel, and Bakelite. Sealing materials were NBR, and Viton.

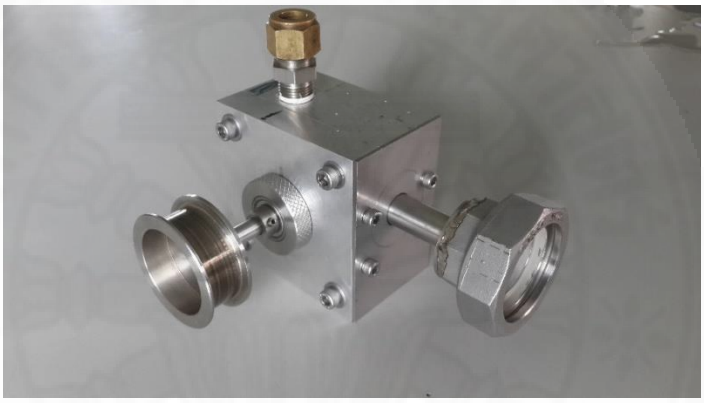

Figure 3.19 1AM expander.

At the exit port, the discharged diameter was enlarged from 5 mm (for the original GAST 1AM air motor) to 14 mm (for the 1AM expander. The exhaust port cross section area was increased by 7.84 times. The threaded fitting was replaced with a straight pipe with O-rings as shown in Figure 3.20.

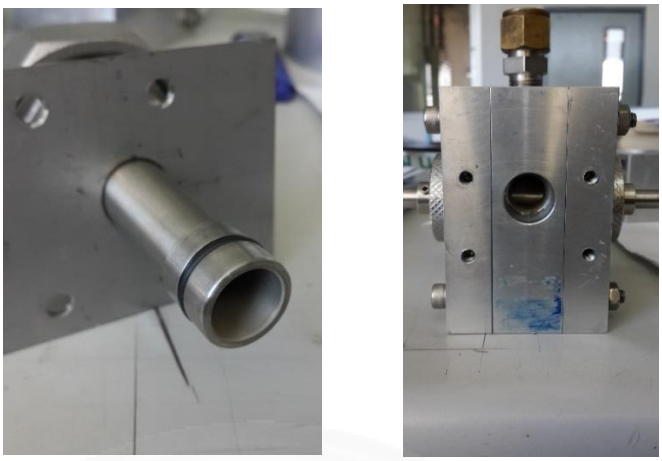

Figure 3.20 Exit port of 1AM expander.

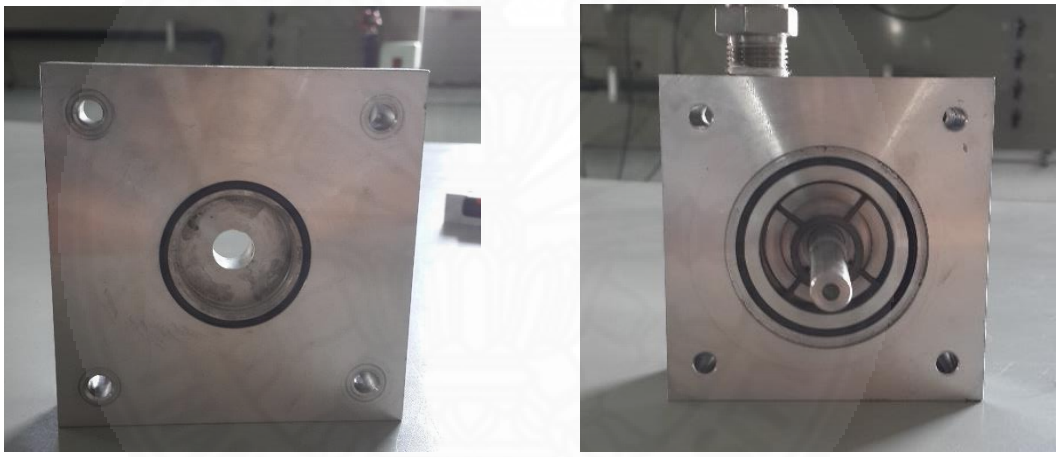

Figure 3.21 1AM expander with Viton O-rings.

For maintenance purposes, the bearing and shaft seal holders were constructed as shown in Figure 3.22. With this design, the bearing or shaft seal could be easily replaced. The geometry drawing of the 1AM expander is provided in Appendix B.

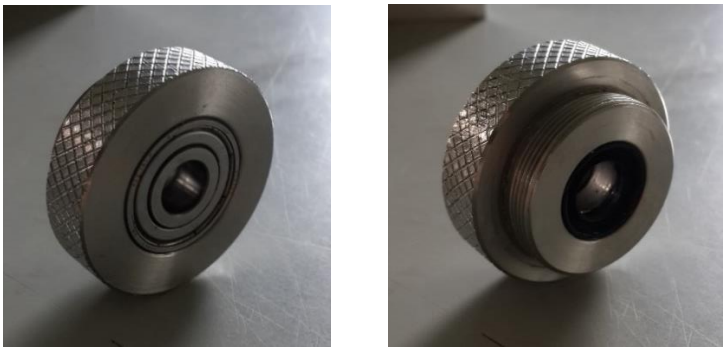

Figure 3.22 Bearing and shaft seal holder.

3.4 Instrumentation and system control

The performance of an ORC is defined by the thermal efficiency which is defined as the ratio between the system power output and the thermal energy supplied to the vapour generator. The system power output produced at the expander can be determined by the means of shaft power or electrical power generated. The thermal energy supplied to the vapour generator can be calculated from the mass flow rate of the high pressure and high temperature R141b vapour and its enthalpy.

In order to determine the shaft power, the Prony brake is employed to determine the torque of the expander and it is later used to determine the shaft power. The setup of the Prony brake is shown in Figure 3.23. In order to get an accurate result, electronic scale of the Prony brake was calibrated with the standard weight. The calibration was done following the user manual of the load cell used. The Prony brake was set to make the expander lift the weight when the shaft was rotated. The weight load of the Prony brake was applied at the weight hanger which could be read by the load cell. The weight was increased until the expander failed to operate. At specific weight loads, the rotational speeds were recorded by tachometer Testo 470 in order to calculate the shaft power.

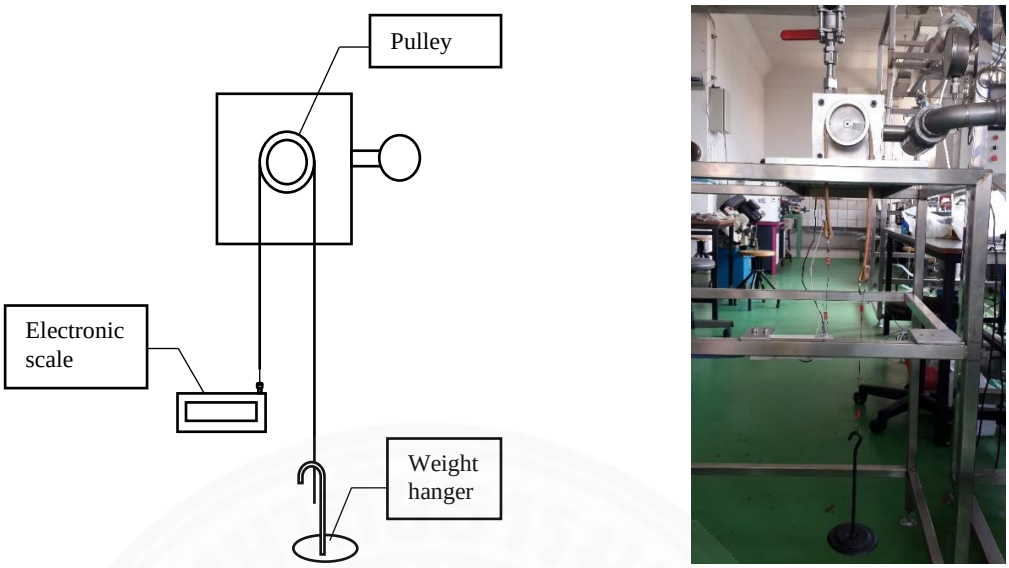

Figure 3.23 Expander with Prony brake.

For electrical power, the expander was connected to a DC generator (modified a brushless AC servo motor) as shown in Figure 3.24. The DC electronic load (ITECH IT8512) was used as an electrical load. The load on the generator was controlled by adjusting the resistance value of the electronic load. At specific loads, the voltage, current, and rotational speed were recorded.

Figure 3.24 Expander with generator.

To control the operating condition of the system, the saturation temperature and saturation pressure of the working fluid at the vapour generator and the condenser needed to be measured. In order to obtain the thermal energy supplied to the vapour

generator, the mass flow rate produced by the vapour generator needed to be measured. To obtain the accurate results, the measuring devices and technique of implementing the experimental should be reliable.

To obtain reliable temperature values, a type–K thermocouple probe, which was used to monitor the temperature at the point of interest as shown in Figure 3.1, was calibrated precisely by comparing it with a high precision mercury thermometer. The reference point at 0°C was obtained by using ice water, while the reference point at 100°C was obtained by the boiling water at the atmospheric pressure. The thermocouple probe had an uncertainty of ± 0.5°C. To achieve the desired point of temperature, the PID logic temperature controllers, SHINKO digital meter JCS–220, were used.

Two pressure transducers were used to detect the pressure at points of interest as shown in Figure 3.1. The pressure transducers were calibrated with a high precision dead weight tester. The atmospheric pressure was indicated by a high precision mercury barometer. From the calibration of the pressure transducers, their uncertainty of reading value was about ±1.0 of full scale.

The working fluid level inside the vessels could be observed by an attached sight glass. The mass flow rate of working fluid from the vapour generator could be determined by observing the dropping rate during a certain time interval. The mass flow rate was later used to calculate the heat supplied to the vapour generator and the thermal efficiency of the system.

3.5 Conclusion

This chapter provided the details of design and construction of an ORC experimental rig. The design concept of each components was explained. The instrumentation and controlling system are designed precisely in order to easily observe the system performance at various operating conditions.

The ORC experimental test rig was developed for conducting the experiment. The purpose is to observe the performance of the sliding vane expander at the various operating conditions. The effect of operating condition change on the sliding vane expander will later be discussed and concluded.

Chapter 4
Result and discussion

This chapter presents the experimental performance of the experimental ORC system. Two expanders, a 2AM expander and a 1AM expander, were used. The working fluid used was R141b. The experimental system was tested with saturation temperature at the vapour generator between 70 and 100°C. The saturation temperature at the condenser was between 34 and 42°C. Power output from these expanders was obtained by using the Prony brake (for both 2AM and 1AM expanders) and by using DC generators (for 1AM expander only).

4.1 Performance analysis

Performance of the ORC system is defined as the thermal efficiency. It can be estimated from the ratio between the power output at the expander and the thermal energy input at the vapour generator as shown

$$\eta = \frac{\dot{W}_{ex}}{\dot{Q}_{gen}} \times 100 \tag{4.1}$$

Where η Thermal efficiency of the ORC system (%)

$\dot{W}_{ex}$ Power output from the expander (kW)

$\dot{Q}_{gen}$ Heat input to the vapour generator (kW)

Heat addition to the vapour generator can be determined by

$$\dot{Q}_{gen} = \dot{m}_{sys} \times (h_{g@gen} - h_{f@con}) \tag{4.2}$$

Where $\dot{m}_{sys}$ Mass flow rate of the ORC system (kg/s)

$h_{g@gen}$ Enthalpy of the fluid (saturated vapour) at the vapour generator exit (kJ/kg)

$h_{f@con}$ Enthalpy of the fluid (saturated liquid) at the vapour generator inlet which is equal to that at condenser outlet (kJ/kg)

The shaft power output produced at the expander can be estimated from the rotational force as

$$\dot{W}_{ex} = (\frac{2 \times \pi \times n}{60}) \times \tau_{ex} \tag{4.3}$$

Where τ_{ex} Torque on the expander's shaft (N·m)
n Rotational speed of the expander (rpm)

To determine the torque of the expander, a Prony brake is applied. The torque can be calculated by the rotational force and the radius of the expander's pulley. The rotational force is the subtraction of the weight load and weight read from the electronic scale at the one end of the brake. The diagram of the Prony brake is shown in Figure 4.1.

$$\tau_{ex} = r \times (F_1 - F_2) \tag{4.4}$$

Where F_1 Weight load at the weight hanger (N)
F_2 Weight read from the electronic scale (N)
r Radius of the pulley (m)

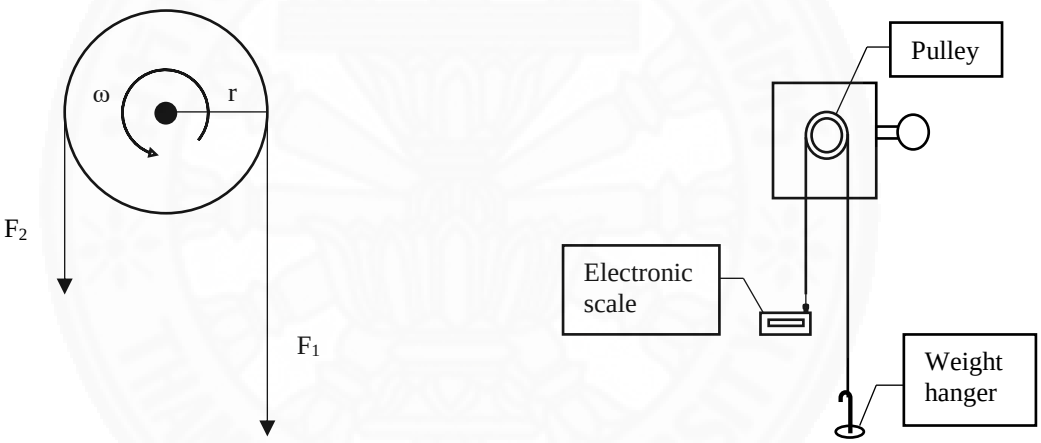

Figure 4.1 Prony brake.

4.2 Performance of 2AM expander by using Prony brake

Variation of the expander performance with Rotational speed

To perform this test, saturation temperature of the vapour generator was maintained at 90°C while the condenser pressure was maintained at 1.08 bar (saturation temperature of 34°C). The weight load was applied to the Prony brake until the expander failed to operate. Torque and rotational speed were recorded at various loads applied. Torque, shaft power, mass flow rate, heat input, and thermal efficiency are plotted against the rotational speed as shown in Figure 4.2.

It can be seen from Figure 4.2a that when the load is increased, the torque produced by the expander increases linearly with a decrease of the rotational speed.

This means torque is inversely proportional to the rotational speed. The maximum torque of 0.52 N·m is obtained at a rotational speed of 3,157 rpm. It can also be seen when the load is increased, the shaft power increases as rotational speed decreases until reaching its maximum value of 185 W at 4,100 rpm. Then, it decreases as rotational speed continues to decrease. It is noted that the maximum shaft power is not obtained at the maximum torque.

Figure 4.2b shows the mass flow rate and the heat input at the vapour generator at various rotational speeds. It is seen that the mass flow rate of the high pressure vapour increases with the rotational speed. When considered precisely, the mass flow rate slightly changes with the rotational speed. As a result, the heat input to the vapour generator slightly increases with rotational speed. Since the heat input to the vapour generator is almost constant, the thermal efficiency curve is similar to that of the shaft power curve as shown in Figure 4.2c. The maximum thermal efficiency of 1.57% is obtained at 4,100 rpm. The maximum shaft power and thermal efficiency indicate the optimal point of this 2AM expander for this particular operation.

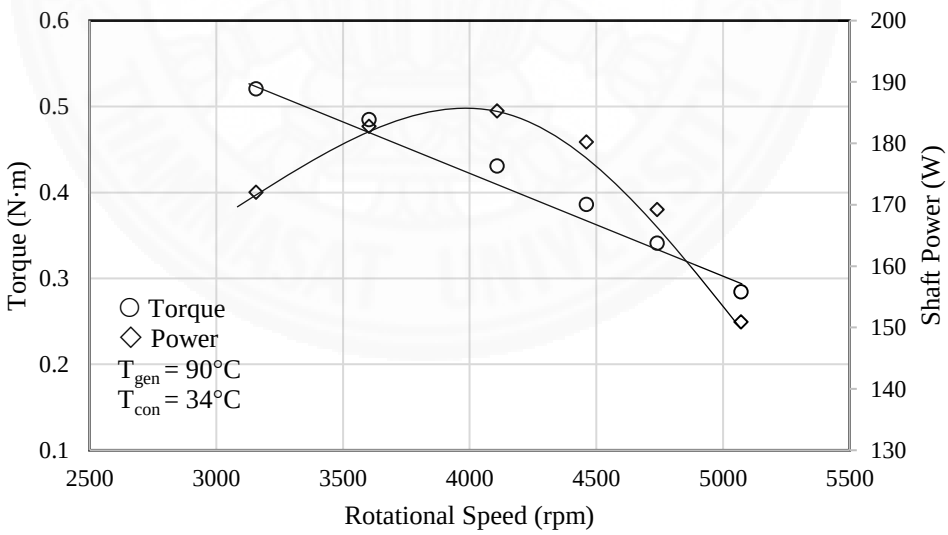

(a) Torque and Shaft Power against Rotational Speed.

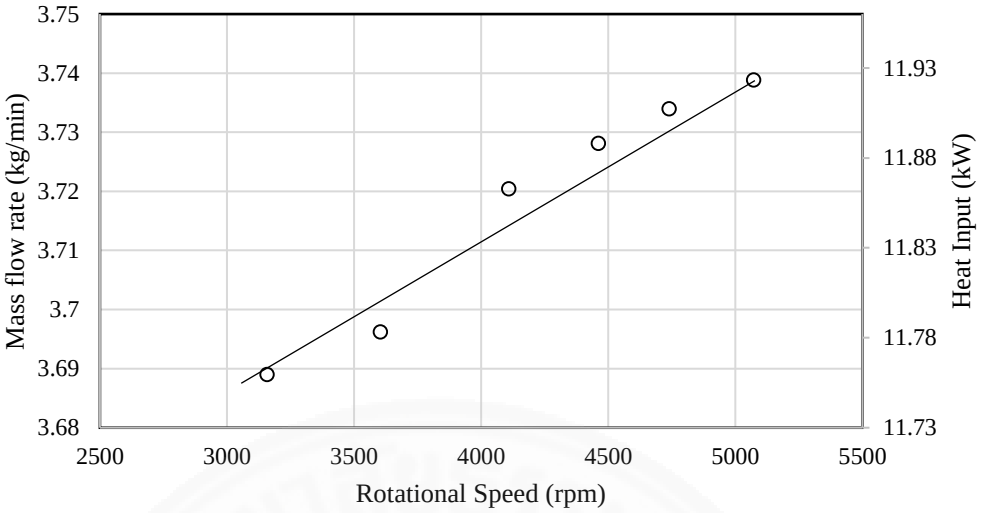

(b) Mass flow rate and Heat Input against Rotational Speed.

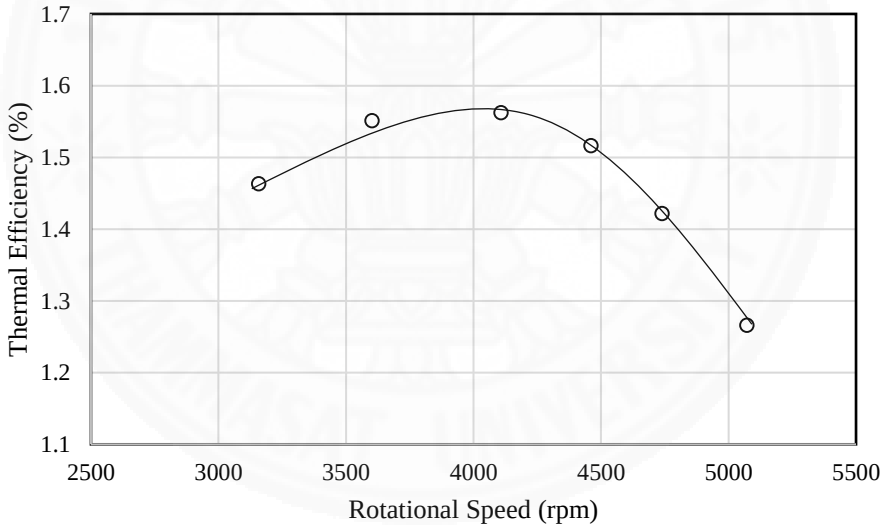

(c) Thermal Efficiency against Rotational Speed.

Figure 4.2 Experimental performance of 2AM expander when the vapour generator is at 90°C and condensation is at 34°C.

Effect of the condenser saturation temperature

The saturation temperature of the vapour generator was maintained constant at 90°C while the condenser pressure was at 1.08, 1.24, and 1.42 bar (saturation temperature of 34°C, 38°C, and 42°C). The torque, shaft power, mass flow rate, heat input, and thermal efficiency are plotted against the rotational speed as shown in Figure 4.3. The increase of the condensation temperature results in the differential temperature between heat source and heat sink of the experimental ORC being reduced. This causes the reduction of torque and shaft power at identical rotational speed as shown in Figure 4.3a and 4.3b.

It can be seen from the Figure 4.3c that mass flow rate and heat input at the vapour generator are dependent on the rotational speed only. Due to the reduction in the shaft power while the heat input to the vapour generator is kept constant, the thermal efficiency is reduced as the condensation temperature is increased. The thermal efficiency curve is shown in Figure 4.3d.

Referring to Figures 4.3b and 4.3d, the maximum value of the shaft power and the thermal efficiency decrease as the condensation temperature is increased. The optimal point (for each curve) decreases linearly with an increase in condensation temperature as shown by the optimal line operation.

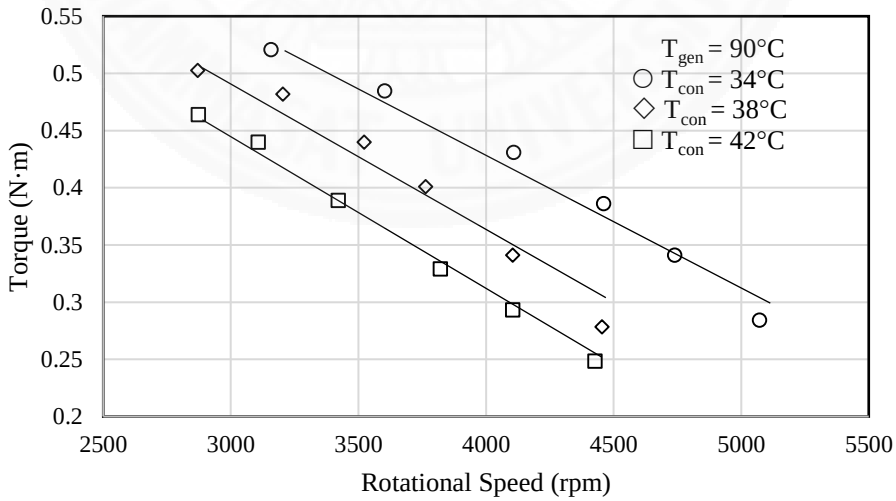

(a) Torque against Rotational Speed.

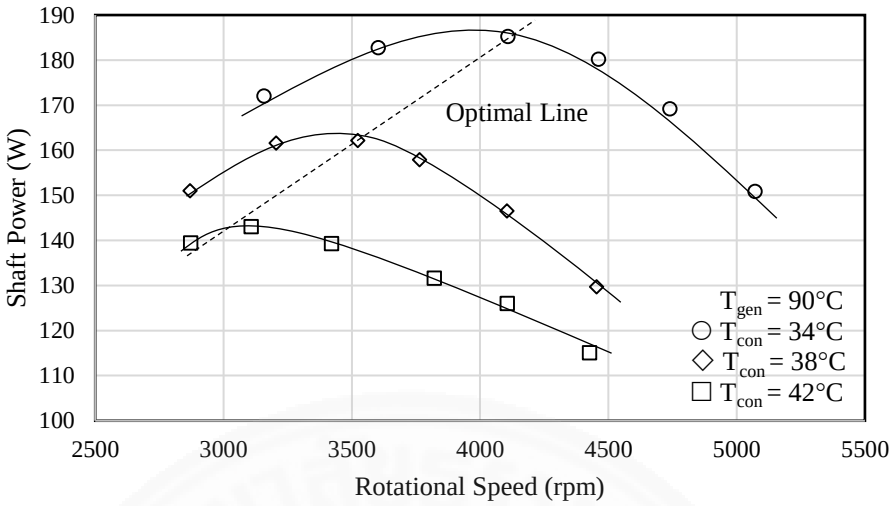

(b) Shaft Power against Rotational Speed.

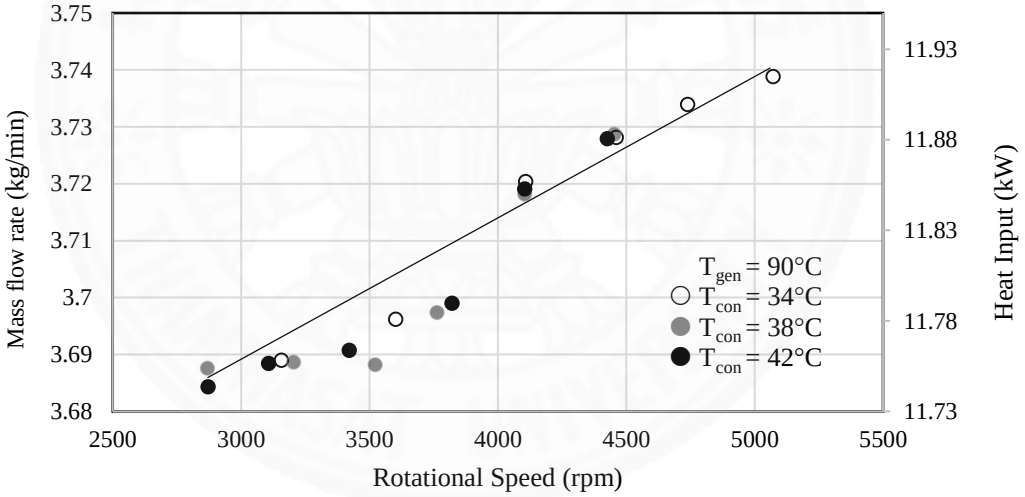

(c) Mass flow rate and Heat Input against Rotational Speed.

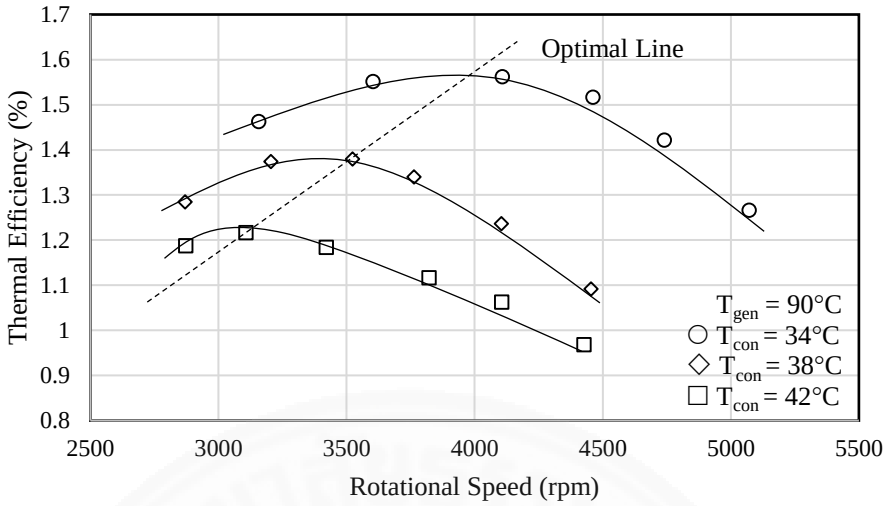

(d) Thermal Efficiency against Rotational Speed.

Figure 4.3 Experimental performance of 2AM expander when the vapour generator temperature is at 90°C and condensation temperature is varied from 34°C to 42°C.

Effect of the vapour generator saturation temperature

The saturation temperature of the vapour generator was at 70°C, 80°C, and 90°C. The condenser pressure was maintained at 1.08 bar (saturation temperature of 34°C). The torque, shaft power, mass flow rate, heat input, and thermal efficiency are plotted against rotational speed in Figure 4.4.

It is found from Figures 4.4a and 4.4b that a decrease in the vapour generator temperature causes the differential temperature between heat source and heat sink to be reduced. This causes a reduction of torque and shaft power at identical rotational speed.

It can be seen from Figure 4.4c that at the identical rotational speed, when the vapour generator temperature is decreased, a decrease in the mass flow rate and the heat input result. One would expect that a better thermal efficiency would be obtained. However, overall, a decrease of the shaft power causes the thermal efficiency to drop as shown in Figure 4.4d.

Referring to Figures 4.4b and 4.4d, the maximum values for the shaft power and the thermal efficiency decrease as the vapour generator temperature is decreased. The

optimal point decreases linearly with a decrease in vapour generator temperature as shown by the optimal line operation.

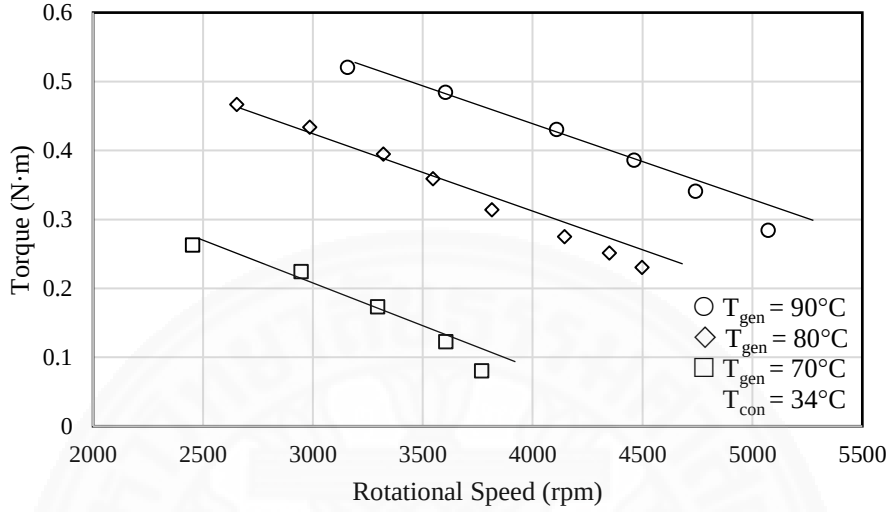

(a) Torque against Rotational Speed.

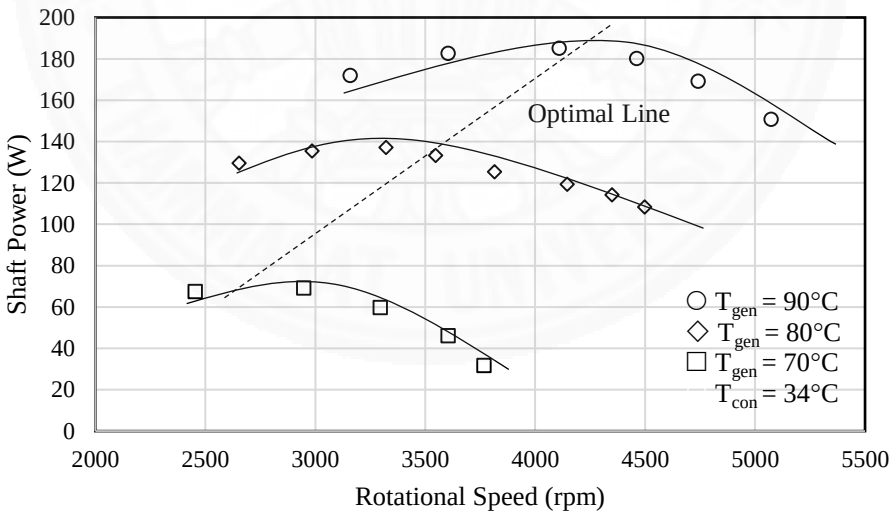

(b) Shaft Power against Rotational Speed.

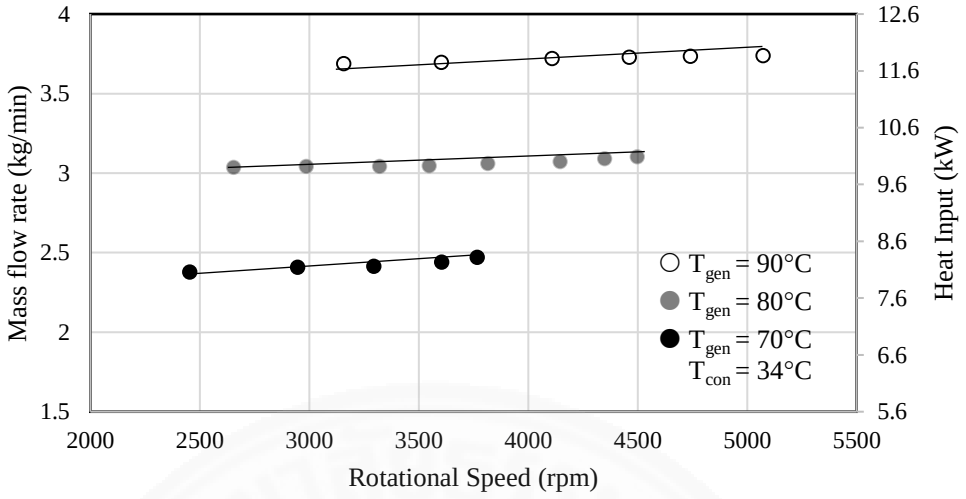

(c) Mass flow rate and Heat Input against Rotational Speed.

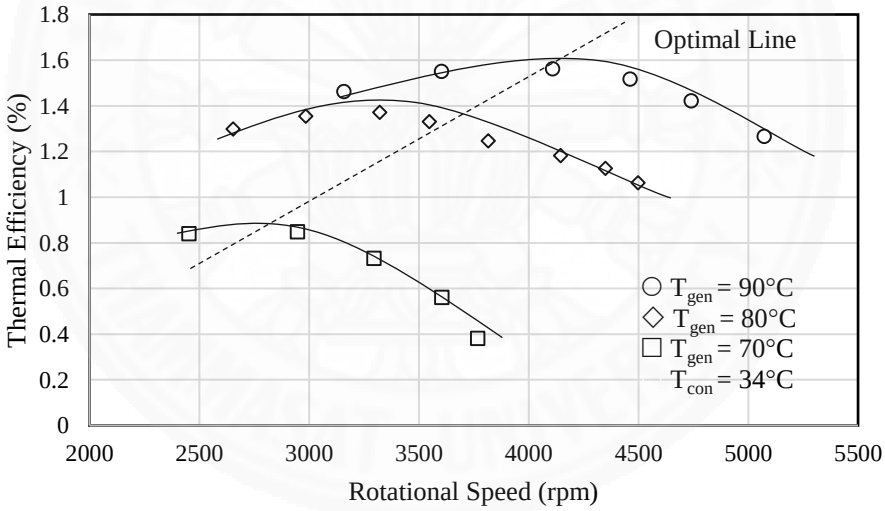

(d) Thermal Efficiency against Rotational Speed.

Figure 4.4 Experimental performance of 2AM expander when the vapour generator temperature is at 70°C, 80°C, and 90°C and the condensation temperature is at 34°C.

From the performance testing of 2AM expander, it can be seen that the variation of rotational speed, condensation temperature, and vapour generator temperature all affect the expander performance. An increase of the differential temperature between heat source and heat sink results in an increase of the expander power and thermal

efficiency. The maximum shaft power of 185 W is obtained at 4,100 rpm and maximum thermal efficiency of 1.57% is obtained at 4,100 rpm. Both are obtained at the vapour generator and condensation temperatures of 90°C and 34°C, respectively.

4.3 Performance of 1AM expander by using Prony brake

The 1AM expanders was tested with the Prony brake. The testing procedures and conditions were very similar. At first, it was tested for the effect of the shaft output (torque and power) with the variation of the speed. The saturation temperature of the vapour generator was maintained 90°C while the condenser pressure was maintained at 1.08 bar (saturation temperature of 34°C). Performance curves are provided in Figure 4.5.

Performance characteristics for torque, shaft power, mass flow rate, heat input at the vapour generator, and thermal efficiency are very similar to those for the 2AM expander. The maximum torque is 0.13 N·m at 5,700 rpm and the maximum power is 82 W at 7,200 rpm for the 1AM expander compared with 0.52 N·m at 3,157 rpm and 185 W at 4,100 rpm for the 2AM expander. The maximum thermal efficiency of 1.3% is obtained at 5,700 rpm for the 1AM expander which is almost 20% higher than 1.57% at 4,100 rpm for the 2 AM expander.

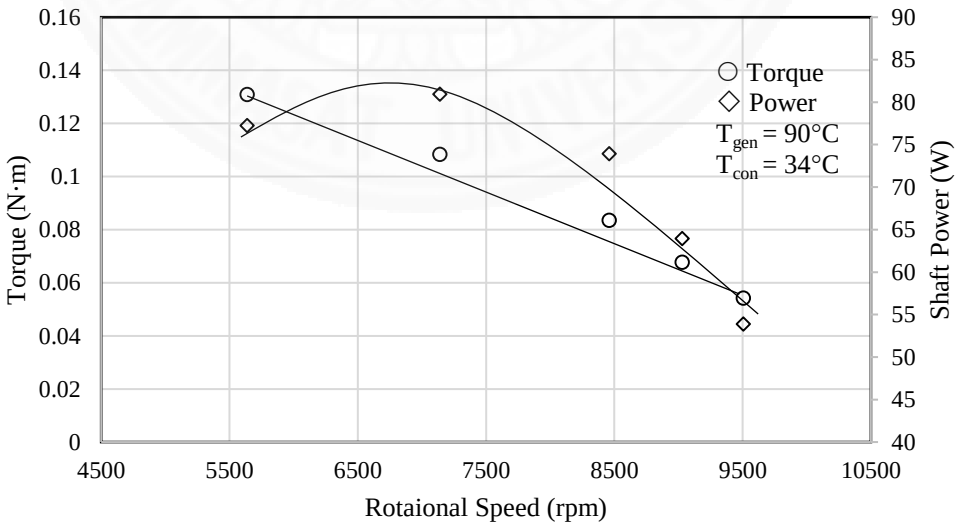

(a) Torque and Shaft Power against Rotational Speed.

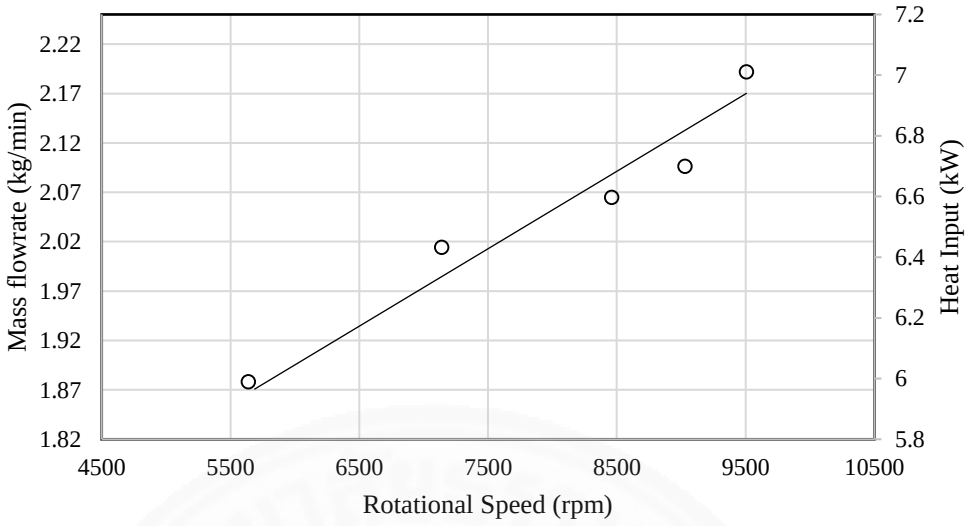

(b) Mass flow rate and Heat Input against Rotational Speed.

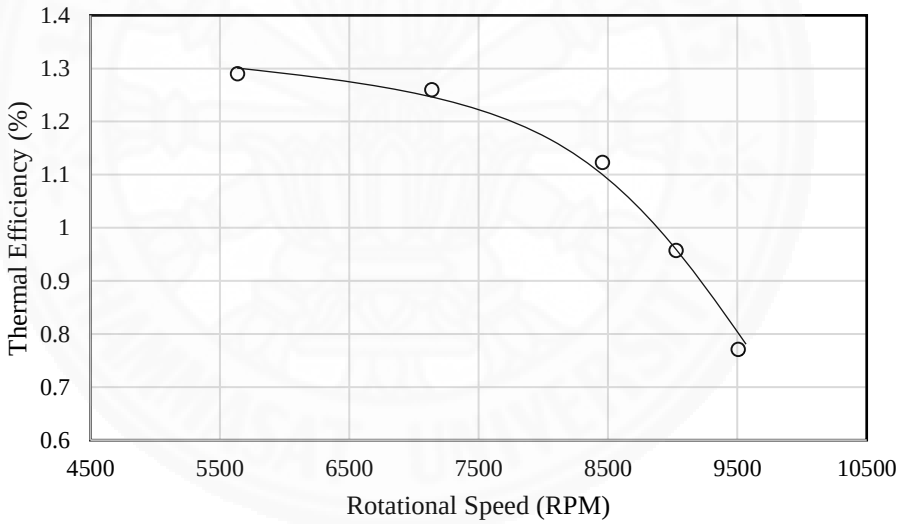

(c) Thermal Efficiency against Rotational Speed.

Figure 4.5 Experimental performance of 1AM expander when the vapour generator is at 90°C and condensation is at 34°C.

Effect of the saturation temperatures at the condenser and at the vapour generator to the performance of 1AM expander are presented in Figures 4.6 and 4.7.

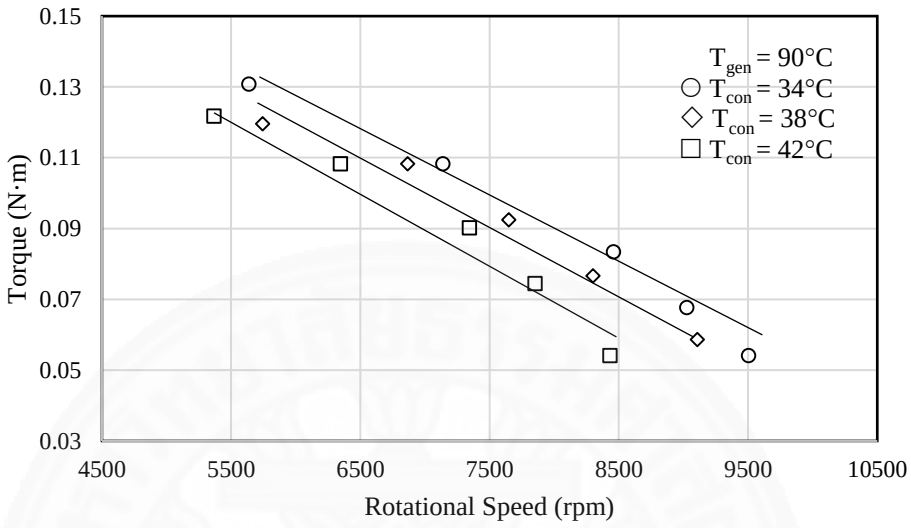

(a) Torque against Rotational Speed.

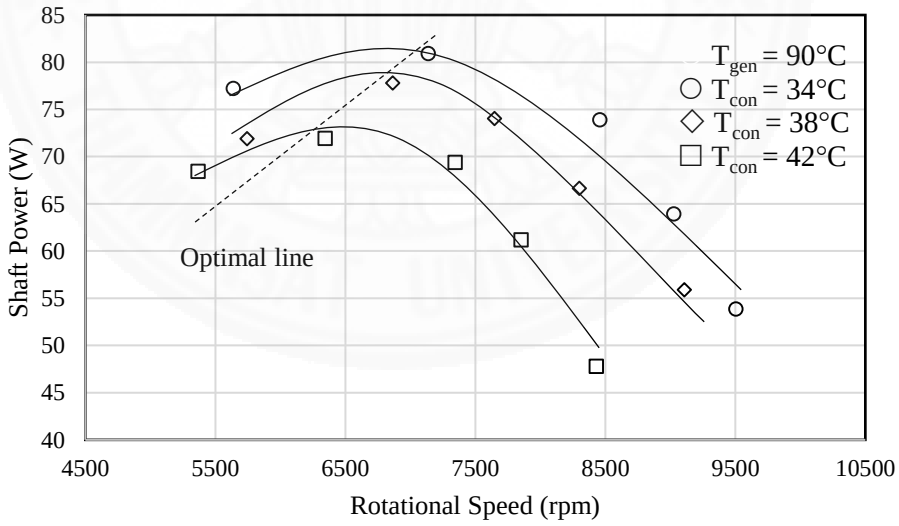

(b) Shaft Power against Rotational Speed.

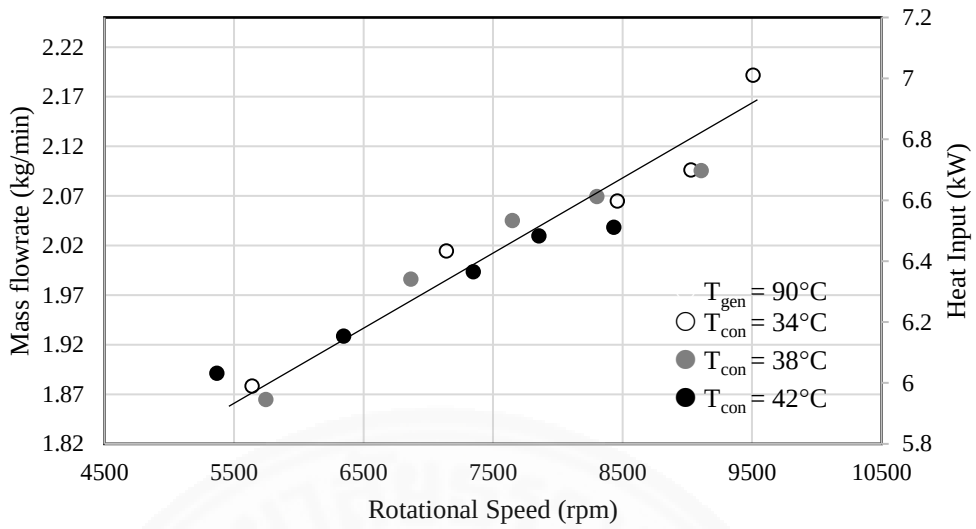

(c) Mass flow rate and Heat Input against Rotational Speed.

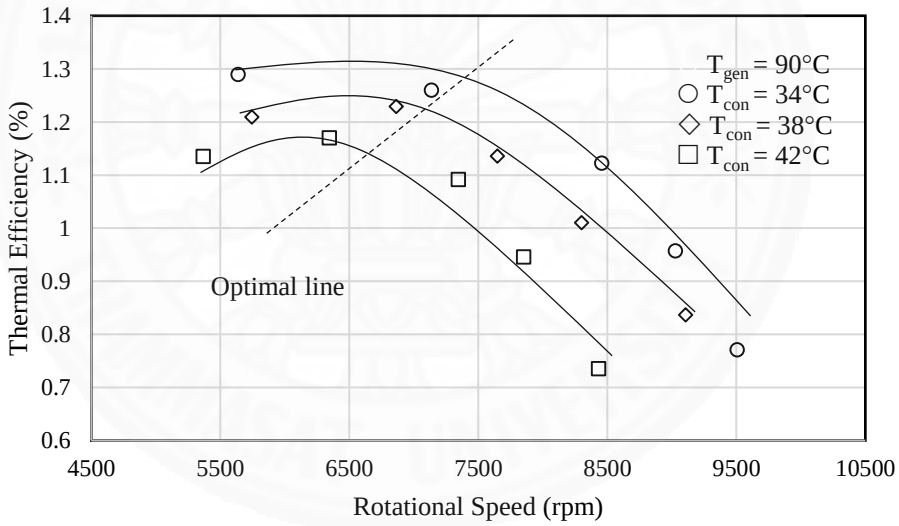

(d) Thermal Efficiency against Rotational Speed.

Figure 4.6 Experimental performance of 1AM expander when the vapour generator temperature is at 90°C and condensation temperature is varied from 34°C to 42°C.

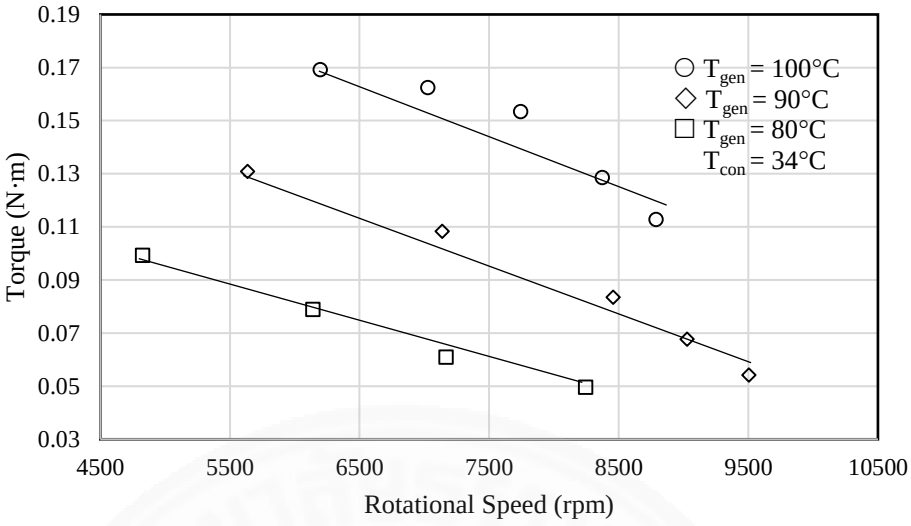

(a) Torque against Rotational Speed.

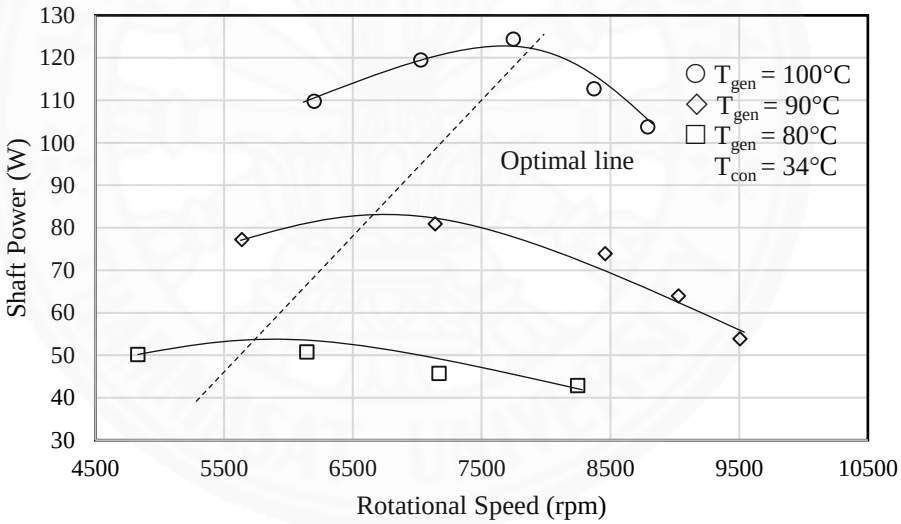

(b) Shaft Power against Rotational Speed.

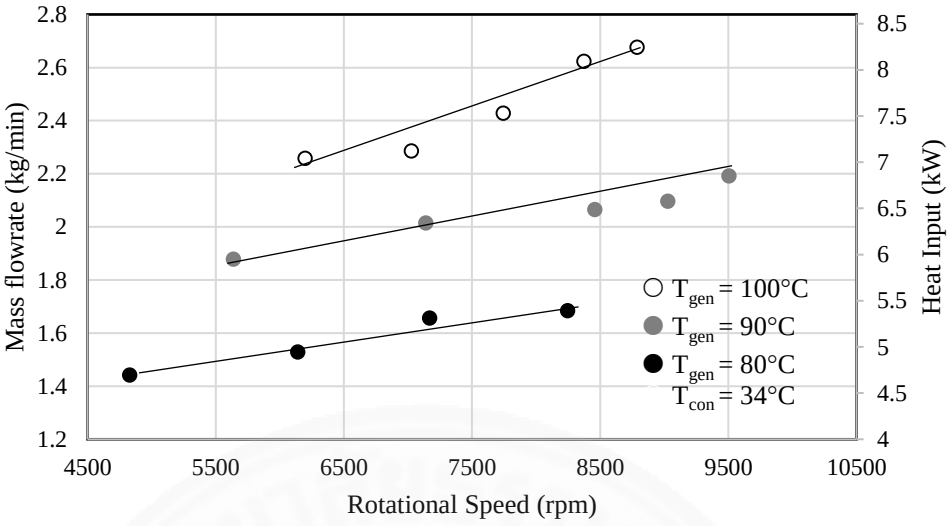

(c) Mass flow rate and Heat Input against Rotational Speed.

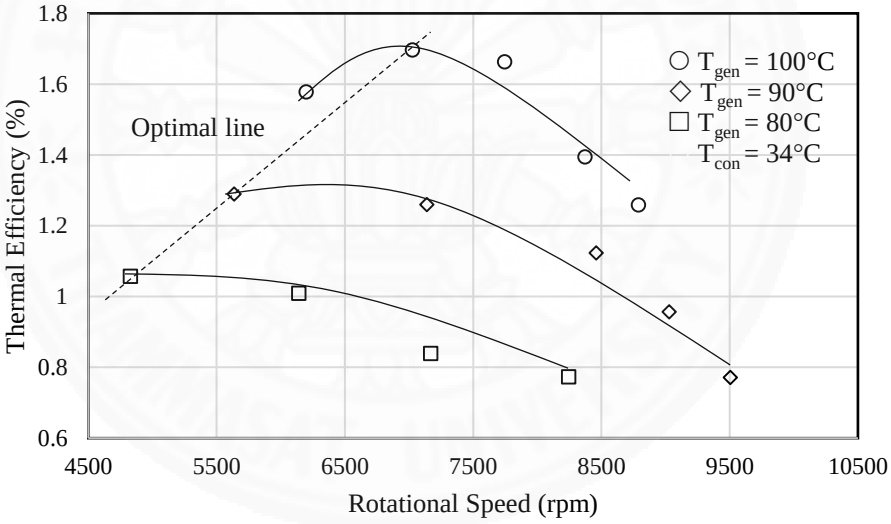

(d) Thermal Efficiency against Rotational Speed.

Figure 4.7 Experimental performance of 1AM expander when the vapour generator temperature is at 80°C, 90°C, and 100°C and the condensation temperature is at 34°C.

The maximum shaft power of 124 W is obtained at 7,700 rpm. And the maximum thermal efficiency of 1.7% is obtained at 7,000 rpm. Both maximum shaft power and thermal efficiency are obtained at the vapour generator temperature of 100°C and condensation temperature of 34°C. Table 4.1 shows the maximum torque and the maximum power for both 1AM and 2AM expanders.

Table 4.1 The maximum torque, power, and thermal efficiency for both 1AM and 2AM expanders.

		1AM expander			2AM expander		
Temperature (°C)		Torque (N·m)	Power (W)	Thermal efficiency (%)	Torque (N·m)	Power (W)	Thermal efficiency (%)
Generator	Condenser						
90	34	0.13 (5,700)	82 (7,200)	1.3 (5,700)	0.52 (3,157)	185 (4,100)	1.57 (4,100)
100	34	0.17 (6,200)	124 (7,700)	1.7 (7,000)	–	–	–

4.4 Performance of 1AM expander by using DC generator

To perform this test, the 1AM expander was coupled with a DC generator. The electrical power generated was supplied to the electronic load, ITECH model IT8512. The load was adjusted by adjusting the Resistance value in the electronic load.

To compare the results from the Prony brake and from electrical power, their performance curves are plotted at each particular operating condition as shown in Figure 4.8. The operating condition was set at the vapour generator temperature of 100°C, while the condenser pressure was maintained at 1.08 (saturation temperature of 34°C).

Figure 4.8 shows shaft power output obtained from the Prony brake and from electrical power against rotational speed. It can be seen that the electrical power produced by the DC generator is around 10% less than the shaft power produced by the DC generator. From this, it may be said that, efficiency of the DC generator is around 90%.

It can also be seen that the maximum point for the power from the Prony brake occurred at around 1,000 rpm higher than that for the electrical power generated from the DC generator. This difference is because of the variation of the efficiency for the DC generator as shown in Figure 4.9. It must be noted than the DC generator used was

modified from a second hand brushless AC servo motor because it is locally available at a reasonable low cost.

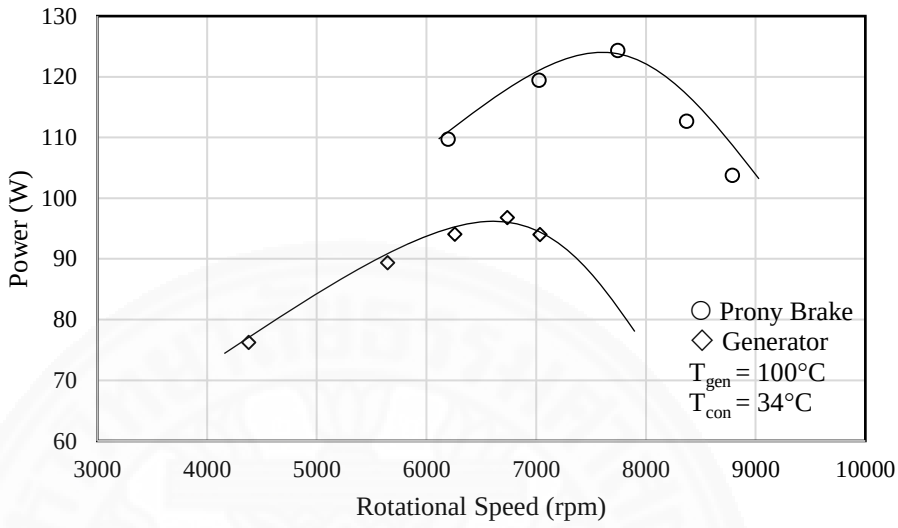

(a) Comparison of the power output when the vapour generator temperature is 100°C and the condensation temperature is at 34°C.

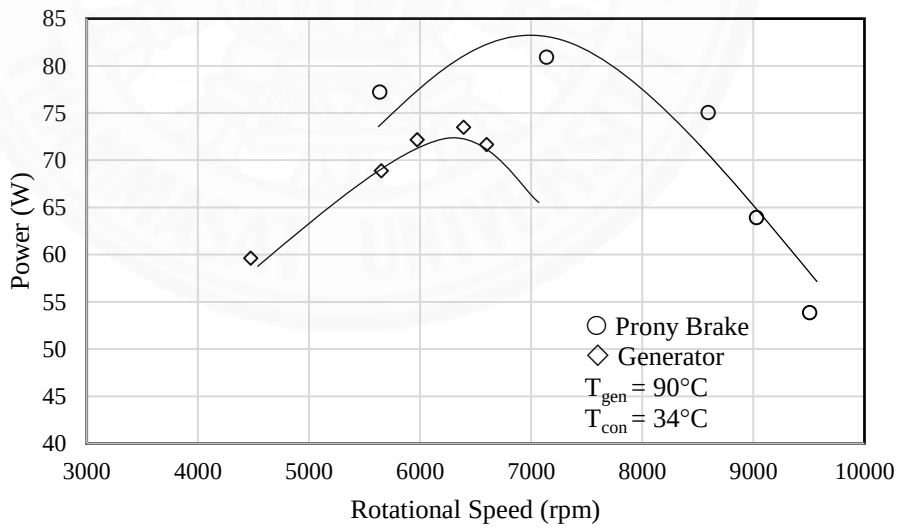

(b) Comparison of the power output when the vapour generator temperature is 90°C and the condensation temperature is at 34°C.

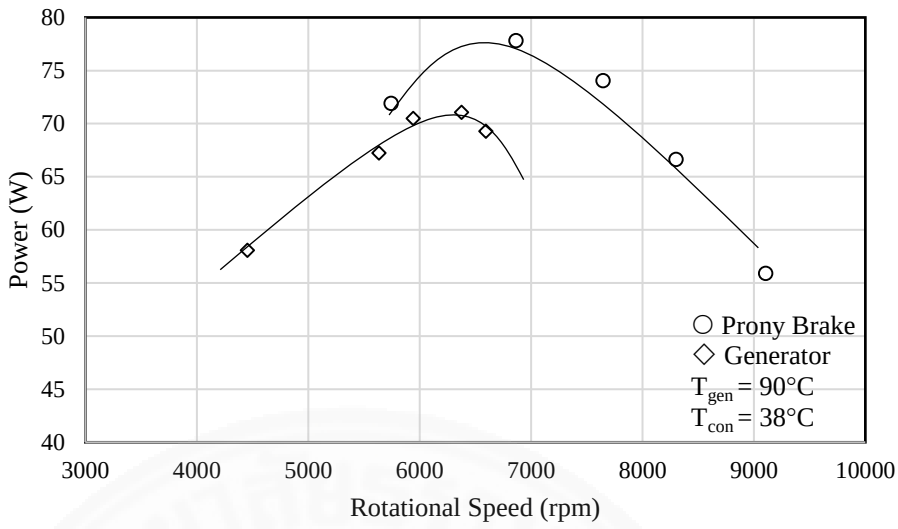

(c) Comparison of the power output when the vapour generator temperature is 90°C and the condensation temperature is at 38°C.

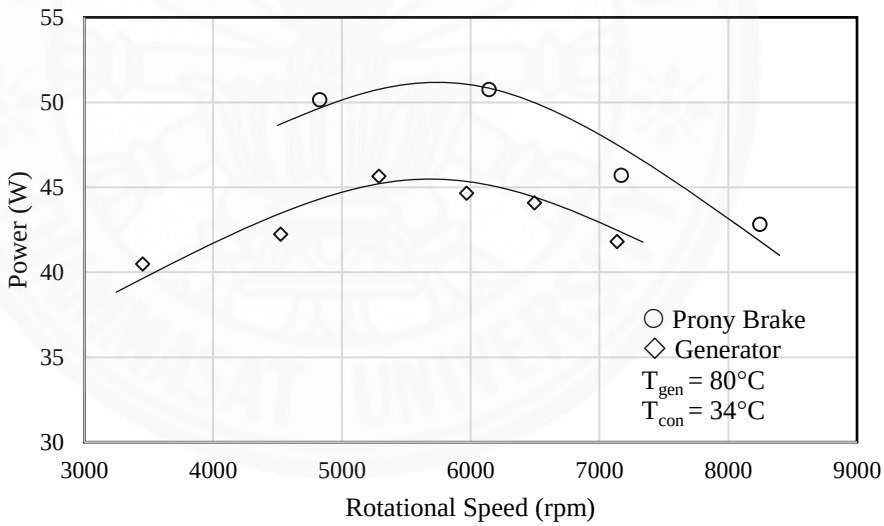

(d) Comparison of the power output when the vapour generator temperature is 80°C and the condensation temperature is at 34°C.

Figure 4.8 Comparison of the power output from 1AM expander obtained by Prony brake and by DC generator.

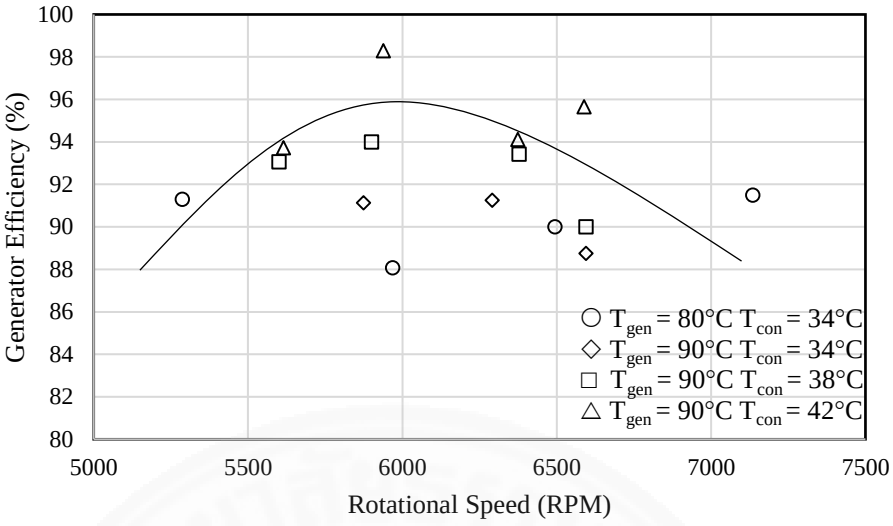

Figure 4.9 Variation of the DC Generator's efficiency with the Rotational Speed.

4.5 Comparison of 2AM and 1AM expander

From the experimental studies of 2AM and 1AM expanders, it was found that both expanders performed acceptably at the various operating conditions. This section provides a performance comparison of these two expanders. Performances obtained by using the Prony brake are only considered. Comparison of the expander performance at identical operating condition, and comparison of the best possible performance of each expander are considered.

This section provides a comparison between the 2AM and the 1AM expander at the same operating condition. This demonstration is implemented at the vapour generator temperature of 90°C and condensation temperature of 34°C. Torque, shaft power, mass flow rate, heat input, and thermal efficiency are plotted against rotational speed as shown in Figure 4.10.

It can be seen from Figure 4.10 that each expanders operates with different rotational speed. The 2AM expander is workable at a rotational speed of around 3,000 to 6,000 rpm while the 1AM expander is workable at around 5,000 to 10,000 rpm. The reason for this difference is due to the design of the air motor. The GAST 2AM air motor has a larger size compare to the GAST 1AM air motor. The GAST 2AM air motor has a maximum rotational speed of 3,000 rpm while the GAST 1AM air motor has a maximum rotational speed of 10,000 rpm.

Figure 4.10a shows that the 2AM expander gives more torque and shaft power output compared to the 1AM expander. Maximum power output from the 2AM expander is 185W at 4,100 rpm while the maximum power output from the 1AM expander is 82W at 7,200 rpm. Also, Figure 4.10b shows that the 2AM expander consumes a higher amount of flow rate compared to the 1AM expander which results in the more heat being required to run the vapour generator.

From Figure 4.10c, it can be seen that the thermal efficiency of the 2AM expander is higher than that of the 1AM expander. The maximum thermal efficiency for the 2AM expander is 1.57% at 4,100 rpm while the maximum thermal efficiency from the 1AM expander is 1.3% at 5,700 rpm.

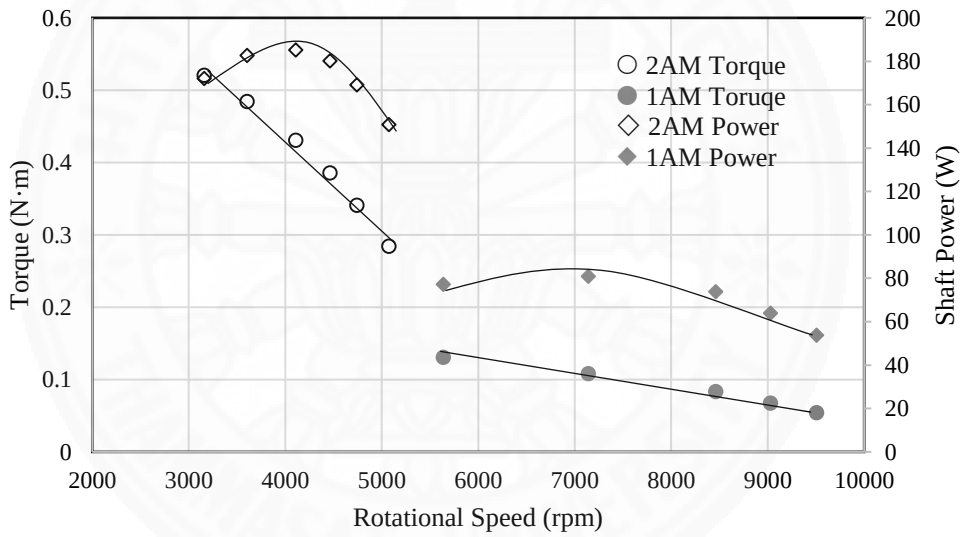

(a) Torque and Power against rotational speed.

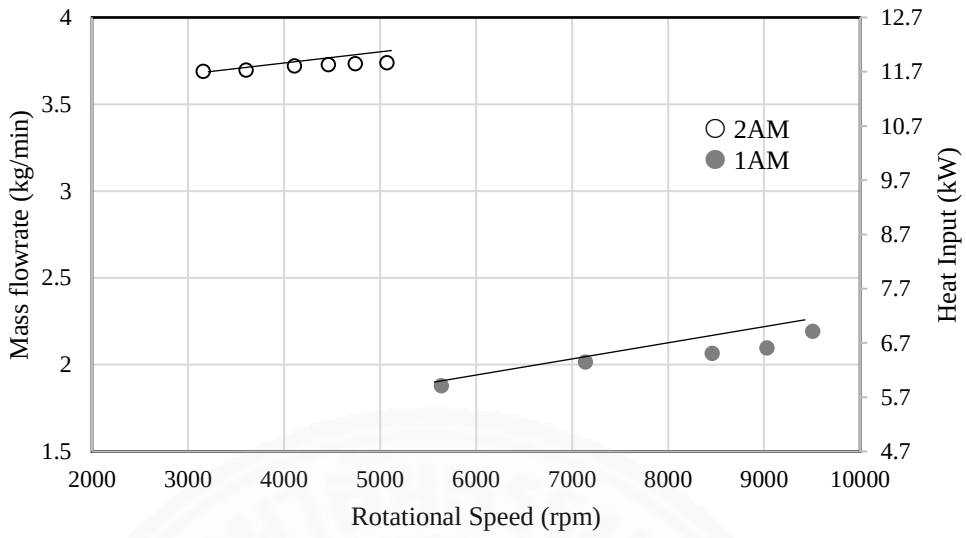

(b) Mass flow rate and Heat Input against Rotational speed.

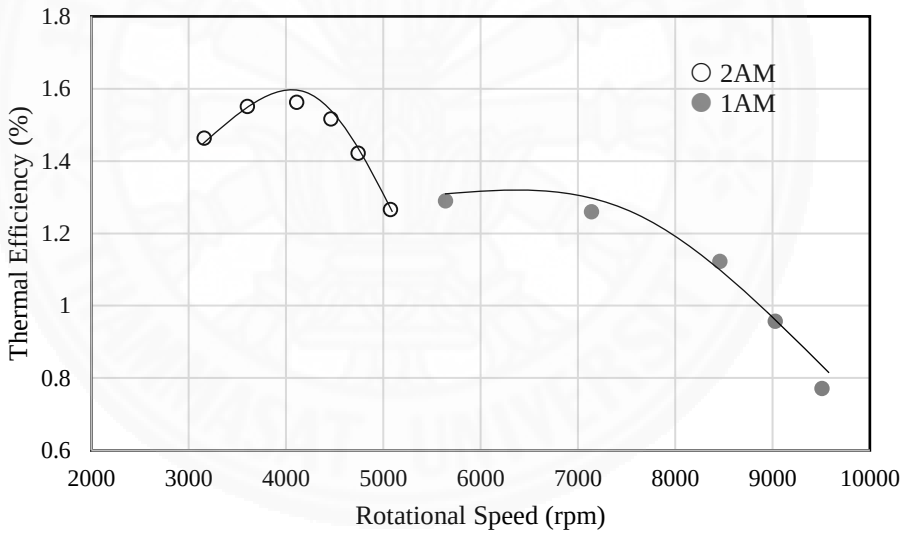

(c) Thermal Efficiency against Rotational speed.

Figure 4.10 Comparing of 2AM and 1AM expander at the vapour generator temperature of 90°C and condensation temperature of 34°C.

As mentioned above, it can be seen that the 2AM expander can produce higher power output and thermal efficiency compared to the 1AM expander at a lower rotational speed. The 2AM expander seems to be more appropriate for real application use when it is applied to a generator. Most of the DC generators that are available in the local market operate at the rotational speed around 3,000 rpm which is closer to the rotational speed of the 2AM expander than the 1AM expander. Even though the 2AM expander consumes more flow rate, which results in a larger amount of heat supplied to the vapour generator, compared to 1AM expander, its rotational speed is reasonable for the real application use.

4.6 Conclusion

In this chapter, the experimental ORC was test with two different expanders, a 2AM and a 1AM expanders. These two expanders were designed and modified based on the commercially available air motors. Working fluid used was R141b. Performance testing of the 2AM and the 1AM expanders was conducted. The power output was determined by two methods: Prony brake and electrical power. This analysis was implemented at various operating conditions. The effects of variation in rotational speed, condensation temperature, and vapour generator temperature on the expander performance were discussed. From the experiment conducted, it was found that:

- Torque, shaft power, thermal efficiency varied significantly with the variation in the rotational speed.
- Increasing the condensation saturation temperature resulted in the shaft power and thermal efficiency being decreased.
- Increasing the vapour generator saturation temperature resulted in the shaft power and thermal efficiency being increased.

From the analysis, a larger differential temperature between heat source (heat supplied vapour generator) and heat sink (cooling water for the condenser) could improve the expander efficiency.

From comparing between the power output by the means of the Prony brake and electrical power, it was found that the electrical power was less than the power

determined by Prony brake method by around 10%. This is due to the efficiency of the DC generator being around 88 to 98%, depending on the rotational speed.

Comparing between the 2AM and the 1AM expander, it was found that the 2AM expander produced more power output compared to the 1AM expander. However, when the 1AM expander was used the vapour generator temperature could be as high as 100°C while it was only at 90°C when the 2AM expander was used. This was due to the limited power of the heaters equipped at the vapour generator. As a result of increasing the vapour generator temperature, the thermal efficiency of the 1AM expander was improved and it was higher than for the 2AM expander. Even though the efficiency of the 1AM expander was higher than the 2AM expander, the 2AM expander was seen to be more appropriate for real applications due to its rotational speed.

Chapter 5
Conclusions and Recommendations

This thesis presents the development of two sliding vane expanders to be used in a micro–scale ORC system. An experimental organic Rankine cycle (ORC) rig was designed and constructed to demonstrate the performance of these two sliding vane expanders. The working fluid used was R141b (Dichlorofluoroethane, $CC_{12}F–CH_3$).

This study emphasized on the development of two sliding vane expanders (2AM and 1AM expanders). They were modified from two commercially available air motors (GAST 2AM and GAST 1AM air motors). The 2AM and 1AM expanders were totally manufactured in–house at the SIIT mechanical engineering laboratory. They were redesigned by keeping the original essential dimensions and operating principles of the original GAST air motors. They were redesigned and modified so that the units were leak proof and suitable to use as an expanders for a micro–scale ORC.

Tests were performed to obtain actual performance and characteristic of these expanders. Two methods of power measurement were employed: Prony brake; and electrical power. The effect of operating conditions on the expander performance was investigated. The vapour generator temperature was varied between 70 to 100°C while the condensation temperature was varied between 34 to 42°C. From the experimental results, it was found that the variation of rotational speed, condensation temperature, and vapour generator temperature affect the expander performance.

- Torque, shaft power output, thermal efficiency varied significantly with the variation in the rotational speed.
- Increasing the condensation saturation temperature resulted in the shaft power output and thermal efficiency being decreased.
- Increasing the vapour generator saturation temperature resulted in the shaft power output and thermal efficiency being increased.

The experimental ORC equipped with 2AM expander produced maximum shaft power output of 185 W with thermal efficiency of 1.57% at the shaft speed of 4,100 rpm. When the vapour generator was 90°C and the condenser was 34°C. The 1AM

expander produced maximum power output of 124 W with thermal efficiency of 1.7% at the shaft speed of 7,700 rpm and 7,000 rpm respectively, when the vapour generator was 100°C and the condenser was 34°C. Although n the thermal efficiency of the 1AM expander was higher than the 2AM expander, the latter was seemed to be more appropriate for real applications due to its rotational speed.

The 1AM expander was also tested with a DC generator to produce DC power. It was found that, at the same rotational speed, electrical power produced was around 90% of the shaft power obtained by the Prony brake. This was due to the efficiency of the DC generator.

Recommendation

This thesis has shown that the sliding vane expander can be successfully developed and tested with a micro–scale ORC system. The expander was workable with the system at the various operating condition. The experimental results show that the expander provided an acceptable performance. However, in the future work some improvement is needed in order to efficiently apply the sliding vane expander to the micro–scale ORC system.

- The power output will be determined by the means of electrical power. It is more realistic for the real application use compared to the means of the Prony brake.
- To apply the expander with the commercial generator, its rotational speed should be reduced to the generator rotational speed (around 3,000 rpm).
- The new expander will keep the design from the 1AM expander, because it has a simpler working mechanism compared to the 2AM expander.
- In order to reduce the rotational speed of the 1AM expander, it will be scaled up to a bigger size, which will result in a reduction of rotational speed.

References

Aphornratana, S., & Sriveerakul, T. (2010). Analysis of a combined Rankine–vapour–compression refrigeration cycle. *Energy Conversion and management*, *51*(12), 2557-2564.

Baek, J. S., Groll, E. A., & Lawless, P. B. (2005). Piston-cylinder work producing expansion device in a transcritical carbon dioxide cycle. Part I: experimental investigation. *International Journal of Refrigeration*, *28*(2), 141-151.

Bao, J., & Zhao, L. (2013). A review of working fluid and expander selections for organic Rankine cycle. *Renewable and Sustainable Energy Reviews*, *24*, 325-342.

Cho, S. Y., & Cho, C. H. (2015). An experimental study on the organic Rankine cycle to determine as to how efficiently utilize fluctuating thermal energy. *Renewable Energy*, *80*, 73-79.

Declaye, S., Quoilin, S., Guillaume, L., & Lemort, V. (2013). Experimental study on an open-drive scroll expander integrated into an ORC (Organic Rankine Cycle) system with R245fa as working fluid. *Energy*, *55*, 173-183.

Hsu, S. W., Chiang, H. W. D., & Yen, C. W. (2014). Experimental investigation of the performance of a hermetic screw-expander organic Rankine cycle. *Energies*, *7*(9), 6172-6185.

Kang, S. H. (2012). Design and experimental study of ORC (organic Rankine cycle) and radial turbine using R245fa working fluid. *Energy*, *41*(1), 514-524.

Lord, R. E. (1984). *Engineering research on positive displacement gas expanders. Phase I technical report* (No. DOE/CE/40652-1). Northern Research and Engineering Corp., Woburn, MA (USA).

Muhammad, U., Imran, M., Lee, D. H., & Park, B. S. (2015). Design and experimental investigation of a 1kW organic Rankine cycle system using R245fa as working fluid for low-grade waste heat recovery from steam. *Energy Conversion and Management*, *103*, 1089-1100.

Nguyen, V. M., Doherty, P. S., & Riffat, S. B. (2001). Development of a prototype low-temperature Rankine cycle electricity generation system. *Applied Thermal Engineering*, *21*(2), 169-181.

Pei, G., Li, J., Li, Y., Wang, D., & Ji, J. (2011). Construction and dynamic test of a small-scale organic rankine cycle. *Energy*, *36*(5), 3215-3223.

Peterson, R. B., Wang, H., & Herron, T. (2008). Performance of a small-scale regenerative Rankine power cycle employing a scroll expander. *Proceedings of the Institution of Mechanical Engineers, Part A: Journal of Power and Energy*, *222*(3), 271-282.

Qiu, G., Liu, H., & Riffat, S. (2011). Expanders for micro-CHP systems with organic Rankine cycle. *Applied Thermal Engineering*, *31*(16), 3301-3307.

Qiu, G., Shao, Y., Li, J., Liu, H., & Riffat, S. B. (2012). Experimental investigation of a biomass-fired ORC-based micro-CHP for domestic applications. *Fuel*, *96*, 374-382.

Smith, I. K., Stosic, N., & Kovacevic, A. (2005). Screw expanders increase output and decrease the cost of geothermal binary power plant systems. *Transactions of Geothermal Resource Council, Reno, NV, September*, 25-28.

Yagoub, W., Doherty, P., & Riffat, S. B. (2006). Solar energy-gas driven micro-CHP system for an office building. *Applied thermal engineering*, *26*(14), 1604-1610.

Yamamoto, T., Furuhata, T., Arai, N., & Mori, K. (2001). Design and testing of the organic Rankine cycle. *Energy*, *26*(3), 239-251.

Yang, B., Peng, X., He, Z., Guo, B., & Xing, Z. (2009). Experimental investigation on the internal working process of a CO 2 rotary vane expander. *Applied Thermal Engineering*, *29*(11), 2289-2296.

Zanelli, R., & Favrat, D. (1994). Experimental investigation of a hermetic scroll expander-generator.

Zheng, N., Zhao, L., Wang, X. D., & Tan, Y. T. (2013). Experimental verification of a rolling-piston expander that applied for low-temperature organic Rankine cycle. *Applied energy*, *112*, 1265-1274.

Appendices

Appendix A

Geometry drawing of the 2AM expander

The geometry drawing of the 2AM expander

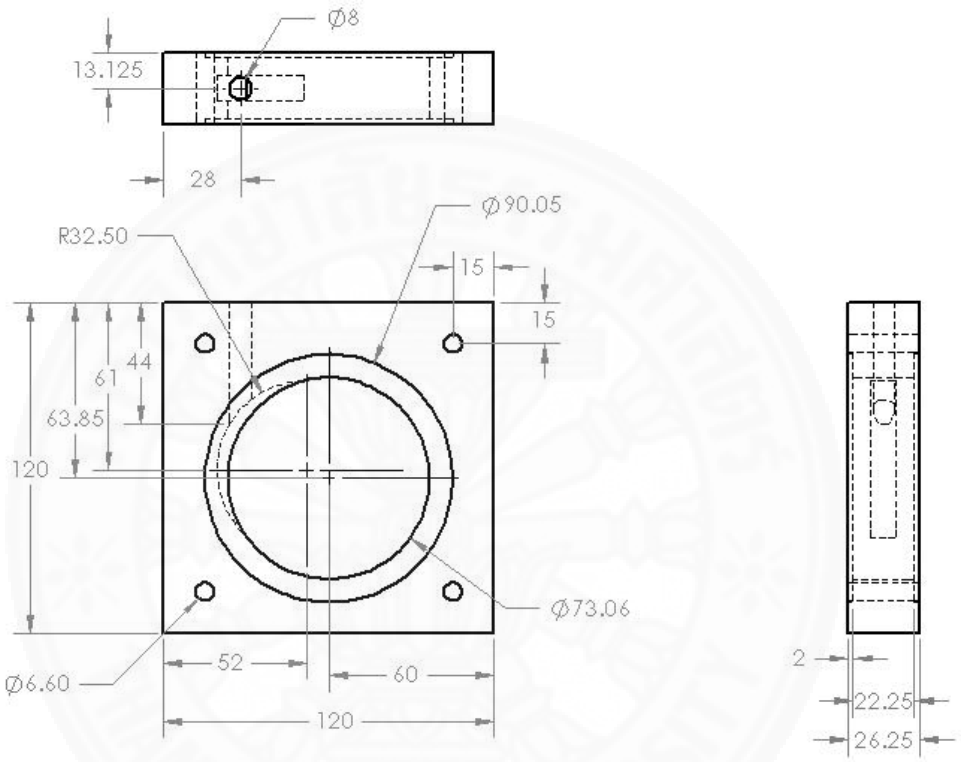

Figure A.1 Body of the 2AM expander.

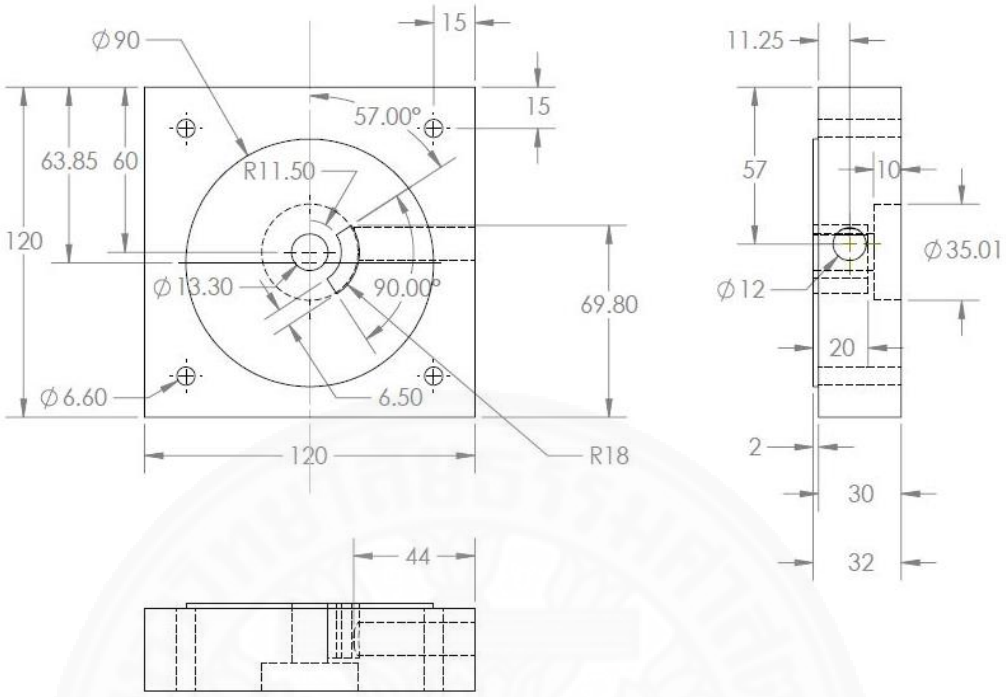

Figure A.2 Covers of the 2AM expander by keeping the geometry from air motor.

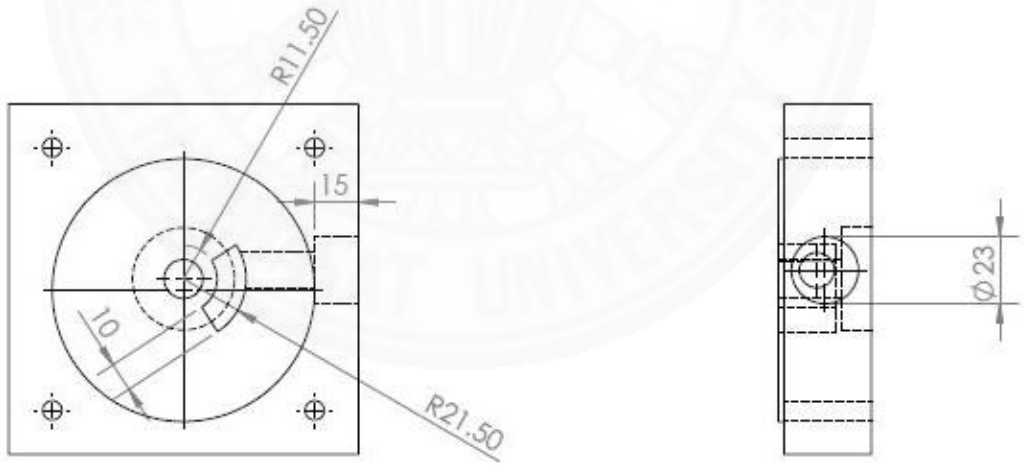

Figure A.3 Cover of the 2AM expander.

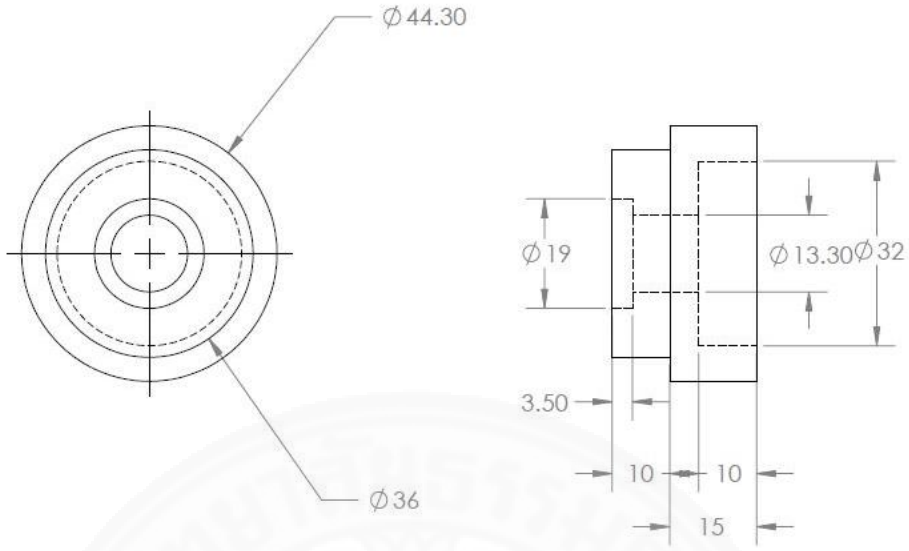

Figure A.4 Bearing and Shaft seal holder of the 2AM expander.

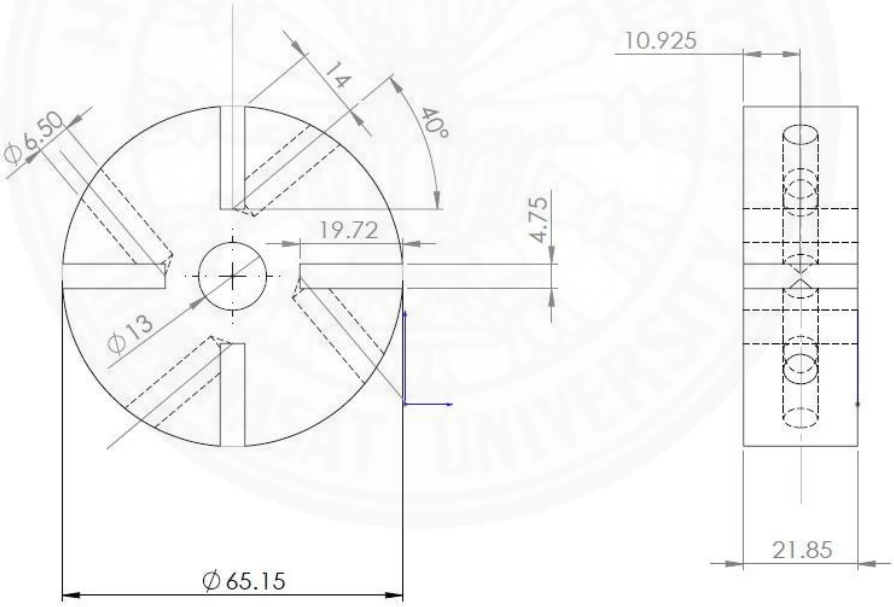

Figure A.5 Original rotor of the 2AM GAST air motor.

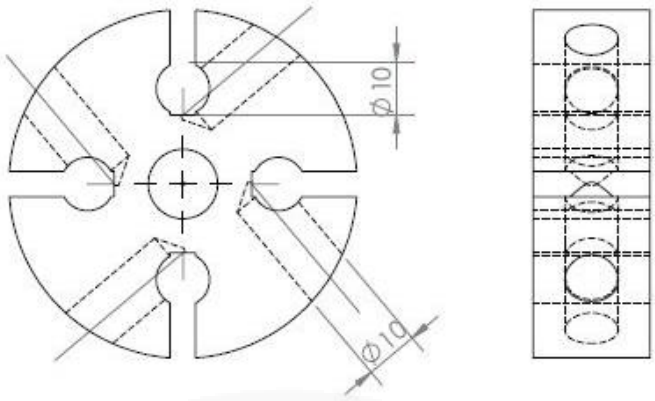

Figure A.6 Stainless steel Rotor of the 2AM expander.

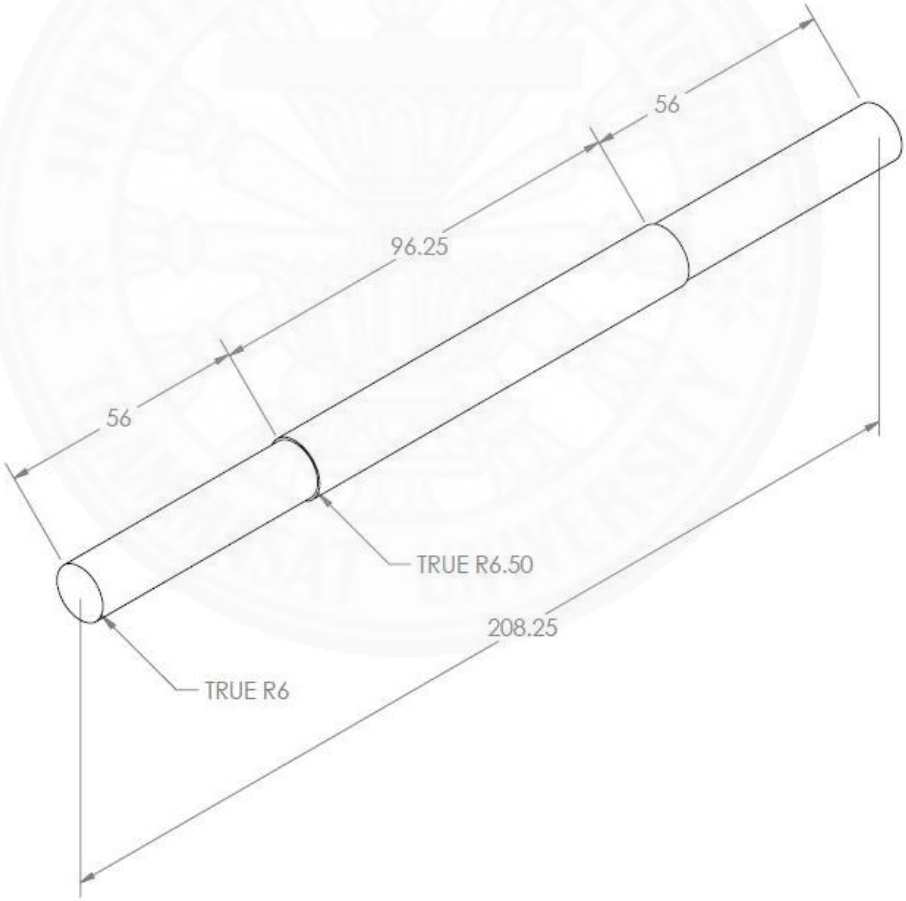

Figure A.7 Shaft of the 2AM expander.

Appendix B

Geometry drawing of the 1AM expander

The geometry drawing of the 1AM expander

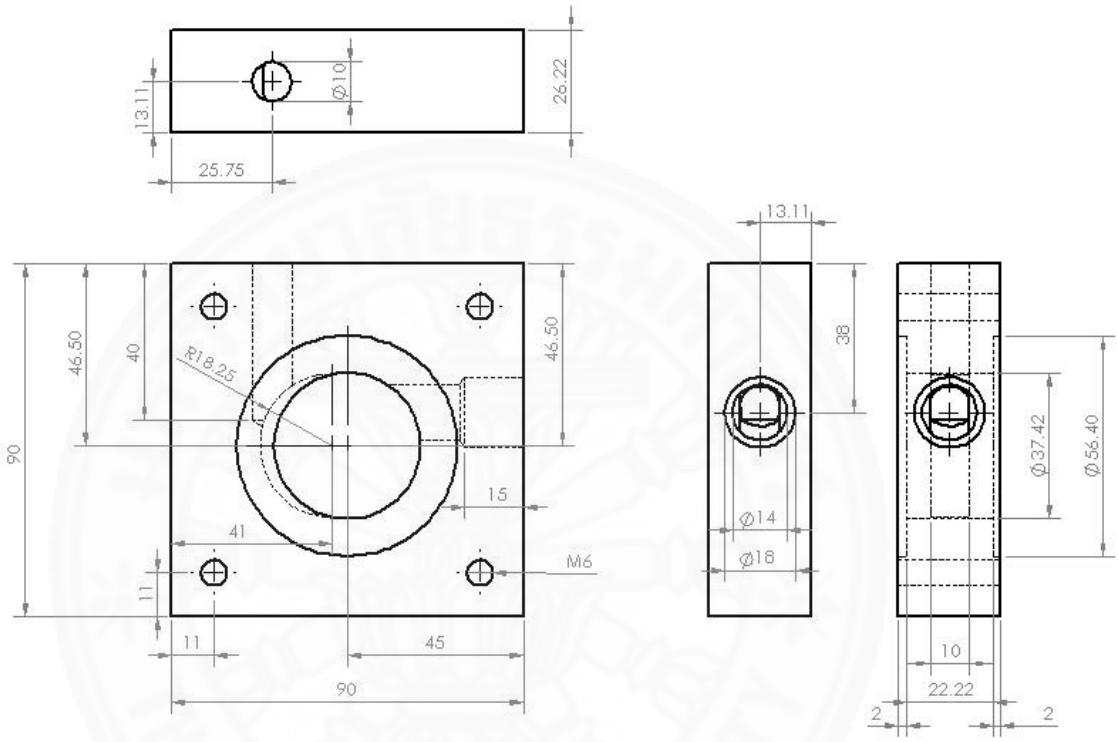

Figure B.1 Body of the 1AM expander.

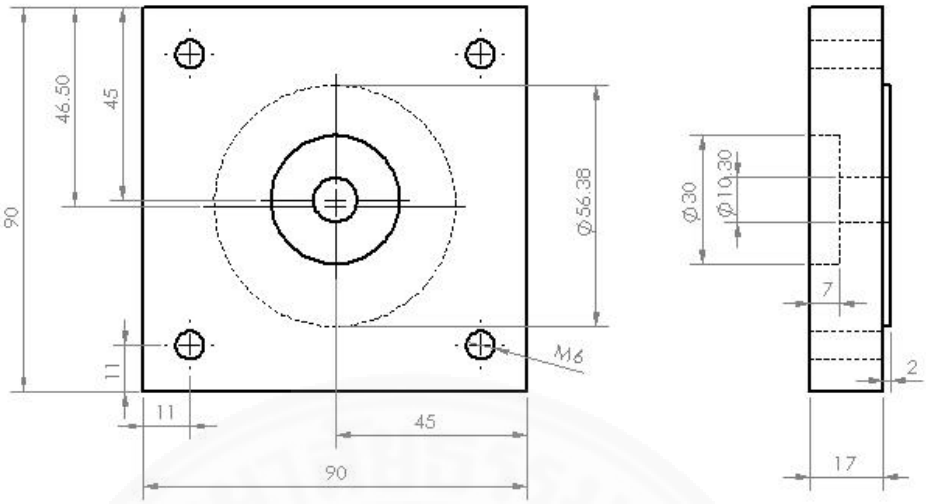

Figure B.2 Cover of the 1AM expander.

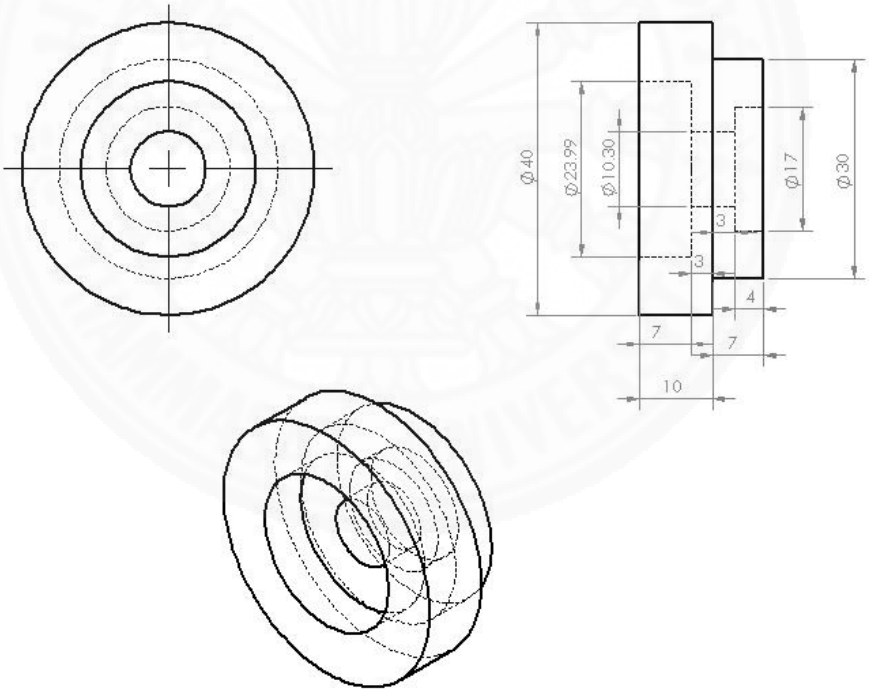

Figure B.3 Bearing and Shaft seal holder of the 1AM expander.

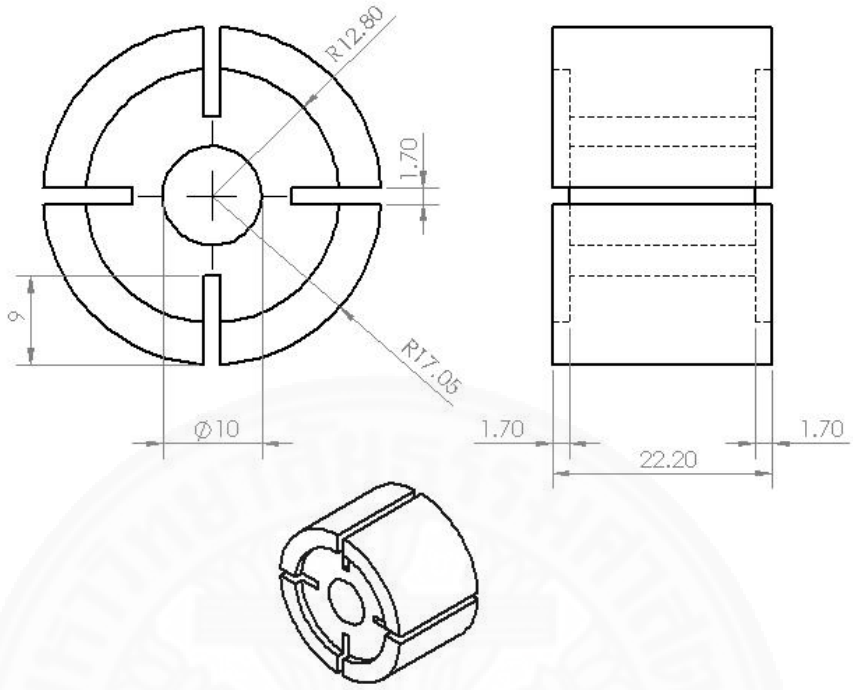

Figure B.4 Rotor of the 1AM expander.

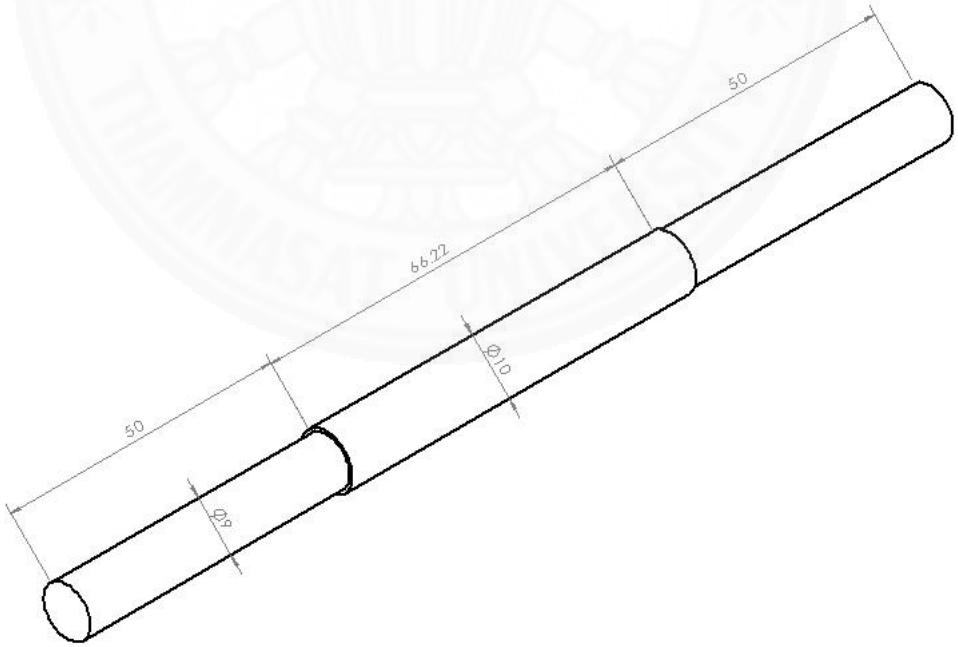

Figure B.5 Shaft of the 1AM expander.